

# Development and Applications of Surface-Confined Transition Metal Complexes

Heterogeneous Catalysis and Anisotropic Particle Surfaces

Kristofer L. E. Eriksson

© Kristofer Eriksson, Stockholm University 2013

Cover picture: Kristofer Eriksson

ISBN 978-91-7447-656-9

Printed in Sweden by US-AB, Stockholm 2013

Distributor: Department of Organic Chemistry, Stockholm University

To my family and friends!

Everyone is a genius.  
But if you judge a fish on its  
ability to climb a tree,  
then it will live its whole life  
believing it is stupid.

*[Albert Einstein]*



# Abstract

The main focus of this thesis has been directed towards developing novel surface-confined transition metal complexes for applications in heterogeneous catalysis and for the preparation of anisotropic particle surfaces. The first part describes the heterogenization of a homogeneous transition metal-based catalyst tetraphenyl cobalt porphyrin (CoTPP) on silicon wafers and on silica particles. The activity in hydroquinone oxidation for the silica particle-immobilized CoTPPs was found to be increased 100-fold compared to its homogeneous congener whereas the silicon wafer-immobilized CoTPPs achieved lower activity due to the formation of clusters of catalyst molecules on the support surface as detected with atomic force microscopy (AFM).

The second part of this thesis describes the development and characterization of anisotropic particle-surfaces by electrochemical site-specific oxidation of surface-confined thiols. Reactive patches or gold gradients could be obtained on the particle surfaces depending on the type of working electrode used and on the electrolyte composition. The particle surface functionalities were characterized with X-ray photoelectron spectroscopy (XPS) and the particle-surface-confined patches and gradients were conjugated with proteins to obtain fluorescence for investigation using fluorescence microscopy. Gold-functionalized siliceous mesocellular foams were further demonstrated to be highly efficient and selective catalysts in the cycloisomerization of 4-alkynoic acids to lactones.

The final part of this thesis describes the preparation and characterization of palladium nanoparticles heterogenized in the pores of siliceous mesocellular foam. The nanoparticles were analyzed with transmission electron microscopy (TEM) and found to have a size of 1-2 nm. Primary- and secondary benzylic- and allylic alcohols were oxidized by the heterogeneous palladium nanoparticles in high to excellent yields using air atmosphere as the oxygen source. The nanopalladium catalyst was used up to five times without any decrease in activity and the size of the nanoparticles was retained according to TEM.



# List of Publications

This thesis is based on the following publications, referred to in the text by their Roman numerals I-VI. The contribution by the author to each publication is clarified in Appendix A.

- I. Performance of a Biomimetic Oxidation Catalyst Immobilized on Silicon Wafers: Comparison with Its Gold Congener**  
Kristofer L. E. Eriksson, Winnie W. Y. Chow, Carla Puglia, Jan-Erling Bäckvall, Emmanuelle Göthelid and Sven Oscarsson  
*Langmuir* **2010**, 26 (21), 16349.
- II. Performance of a Biomimetic Oxidation Catalyst Immobilized on Silica Particles**  
Kristofer Eriksson, Emmanuelle Göthelid, Carla Puglia, Jan-Erling Bäckvall and Sven Oscarsson  
*Under review: J. Catal.* **2012**
- III. Manufacturing of Anisotropic Particles by Site Specific Oxidation of Thiols**  
Kristofer Eriksson, LarsErik Johansson, Emmanuelle Göthelid, Leif Nyholm and Sven Oscarsson  
*J. Mater. Chem.*, **2012**, 22, 7681.
- IV. Electrochemical Synthesis of Gold- and Protein Gradients on Particle Surfaces**  
Kristofer Eriksson, Pål Palmgren, Leif Nyholm and Sven Oscarsson  
*Langmuir* **2012**, 28, 10318.
- V. Electrochemical Preparation of Dispersed Gold Nanoparticles Supported in the Pores of Siliceous Mesocellular Foam: An Efficient Catalyst for Cycloisomerization of 4-Alkynoic Acids to Lactones**  
Kristofer Eriksson, Oscar Verho, Leif Nyholm, Sven Oscarsson and Jan-Erling Bäckvall  
*Manuscript*

**VI. Highly Dispersed Palladium Nanoparticles on Mesocellular Foam: Efficient and Recyclable Heterogeneous Catalyst for Alcohol Oxidation**

Eric Johnston, Oscar Verho, Markus Kärkäs, M. Shakeri, C.-W. Tai, Pål Palmgren, Kristofer Eriksson, Sven Oscarsson and Jan-Erling Bäckvall  
*Chem. Eur. J.* **2012**, *18*, 12202.

Related papers by the author, but not included as part of this thesis:

**A magnetic microchip for controlled transport of attomole levels of proteins**

LarsErik Johansson, Klas Gunnarsson, Stojanka Bijelovic, Kristofer Eriksson, Alessandro Surpi, Emmanuelle Göthelid, Peter Svedlindh and Sven Oscarsson  
*Lab Chip*, **2010**, *10*, 654.

# Table of Contents

Abstract .....	5
List of Publications.....	7
Table of Contents .....	9
Abbreviations .....	12
1.Introduction .....	14
1.1 Catalysis .....	14
1.1.2 Transition Metal Catalysis .....	15
1.1.2.1 Palladium Catalysis - Pd(II) Promoted Oxidations.....	16
1.1.3 Heterogeneous Catalysis.....	18
1.1.3.1 Mechanistic Understanding - Surface Confined Catalysis .....	19
1.1.3.2 Heterogenization of Homogeneous Catalysts.....	21
1.1.3.3 Transition Metal Nanoparticles - Semi Heterogeneous Catalysis.....	23
1.2 Anisotropic Particles.....	26
1.2.1 Preparation of Anisotropic Particles .....	26
1.2.2 Applications of Anisotropic Particles .....	29
1.2.2.1 Anisotropic Particles in Heterogeneous Catalysis.....	29
2. Methods.....	31
2.1 Surface Modifications used in the Thesis .....	31
2.1.1 Introduction of Thiols on Silicon Surfaces in Paper I, III and IV .....	31
2.1.2 Introduction of Thiols on Amino-Functionalized Surfaces in Paper II, III and IV.....	32
2.1.3 Determination of the Thiol Concentration in Paper II, III, IV and V .....	33
2.1.4 Immobilization on Gold Through the Sulfur-Gold Interaction in Paper IV and V .....	34
2.2 Electrochemistry - Principle and Definitions.....	35
2.2.1 Electrochemical Oxidation of Surface Confined Thiols in Paper III.....	37

3. Thesis Aim and Objectives.....	39
4. Performance of a Biomimetic Oxidation Catalyst Immobilized on Silicon Wafers and Silica Particles: Comparison with Its Gold Congener (Paper I and II) .....	40
4.1 Introduction .....	40
4.2 Results and Discussion .....	42
4.2.1 Heterogenization of the Catalyst.....	42
4.2.2 Organization of the Heterogenized Catalysts.....	43
4.2.2.1 Atomic Force Microscopy Study .....	43
4.2.2.2 X-ray Photoelectron Spectroscopy Study.....	44
4.2.3 Catalyst Activity - Reoxidation of Benzoquinone .....	45
4.2.3.1 Turnover Numbers ( $n_{BQ}/n_{CoTPP}$ ).....	46
4.2.3.2 Initial-, Stabilized Turnover Frequencies and Catalyst Reusability.....	47
4.3 Conclusions and Further Perspectives .....	49
5. Manufacturing of Anisotropic Particles by Site Specific Oxidation of Thiols (Paper III) .....	50
5.1 Introduction .....	50
5.2 Results and Discussion .....	51
5.2.1 Preparation of the Anisotropic Particles .....	51
5.2.2 Characterization of the Anisotropic Particles.....	52
5.2.2.1 X-ray Photoelectron Spectroscopy Study.....	53
5.2.2.2 Fluorescence Microscopy Study .....	53
5.2.3 The Conversion Dilemma.....	55
5.3 Conclusions and Further Perspectives .....	56
6. Electrochemical Synthesis of Gold and Protein Gradients on Particle Surfaces and of Dispersed Gold Nanoparticles Supported in the Pores of Siliceous Mesocellular Foam: An Efficient Catalyst for Cycloisomerization of 4-Pentynoic Acids to Lactones (Paper IV and V)57	
6.1 Introduction .....	57
6.2 Results and Discussion .....	58
6.2.1 Particle-Surface-Confined Au <sup>I</sup> Gradients.....	58
6.2.1.1 Preparation of Au <sup>I</sup> and Protein Gradients on Particles .....	58

6.2.1.2 Electrochemical Study - Oxidation of Au <sup>0</sup> to Soluble Au <sup>III</sup> Species .....	59
6.2.1.3 X-ray Photoelectron Spectroscopy Study - Detection of Surface Confined Au <sup>I</sup> .....	60
6.2.1.4 Fluorescence Microscopy Study - Characterization of Particle-Surface-Confined Gradients and Comparison with the Diffusion Layer Thickness .....	61
6.2.2 Surface Confined Au <sup>I</sup> Gradients Modeled on Flat Surfaces .....	63
6.2.2.1 X-ray Photoelectron Spectroscopy Study - Estimation of the Gold Density Profile .....	63
6.2.3 Preparation of Thiol-Stabilized Gold Nanoparticles Supported on Siliceous Mesocellular Foam .....	65
6.2.3.1 Characterization of the Gold Nanoparticles Heterogenized on Siliceous Mesocellular Foam .....	66
6.2.3.2 Cycloisomerization of 4-Pentynoic Acids to Lactones - Heterogeneous Catalysis by Gold Nanoparticles on MCF .....	67
6.3 Conclusions and Further Perspectives .....	70
7. Highly Dispersed Palladium Nanoparticles on Mesocellular Foam: Efficient and Recyclable Heterogeneous Catalyst for Alcohol Oxidation (Paper VI) .....	72
7.1 Introduction .....	72
7.2 Results and Discussion .....	73
7.2.1 Preparation of Palladium Nanoparticles Heterogenized on Siliceous Mesocellular Foam .....	73
7.2.2 Characterization of Palladium Nanoparticles Heterogenized on Siliceous Mesocellular Foam .....	74
7.2.3 Aerobic Oxidation of Alcohols by the MCF-N-Pd(0) Catalyst .....	75
7.2.3.1 Support Study - Oxidation of 1-Phenylethanol with Pd Nanoparticles Heterogenized on MCF and on Silica .....	78
7.3 Conclusions .....	79
8. Concluding Remarks .....	81
Appendix A .....	83
Appendix B .....	84
Acknowledgements .....	85
References .....	88

# Abbreviations

Abbreviations and acronyms are used in agreement with the standard of the subject. Only nonstandard and unconventional ones that appear in the thesis are listed here.

AFM	Atomic force microscopy
BE	Binding energy
BQ	1,4-Benzoquinone
CoTPP	Tetraphenyl cobalt(II)porphyrin
DCM	Dichloromethane
DNA	Deoxyribonucleic acid
DTT	Dithiotreitol
ETM	Electron transfer mediator
FePc	Iron(II)phthalocyanine
GC-MS	Gas chromatography - mass spectrometry
HQ	1,4-Hydroquinone
ICP-MS	Inductively coupled plasma - mass spectrometry
MCF	Siliceous mesocellular foam
NMR	Nuclear magnetic resonance
NP	Nanoparticle
Nu	Nucleophile
PBS	Phosphate buffered saline
PDMS	Polydimethylsiloxane
PDS	Dipyridyl disulfide
SPDP	N-succinimidyl 3-(2-pyridyldithio)-propionate
STM	Scanning tunneling microscopy
TEM	Transmission electron microscopy
TP	Pyridin-2-thione
TOF	Turnover frequency
TON	Turnover number
XP	X-ray photoelectron
XPS	X-ray photoelectron spectroscopy



# 1. Introduction

The understanding of the term *surface-confined transition metal complexes* is that the transition metal complexes are restricted to a surface. In the field of catalysis *surface-confined* aim towards heterogeneous catalysis where the *transition metal complex* is limited to a solid surface where it acts as a catalyst. The surface-confined catalyst can be a solid transition metal surface or it can be a homogeneous transition metal catalyst covalently bound (immobilized or heterogenized) to a solid surface.

The definition of an anisotropic particle surface intends that the particle is irregular in composition. Anisotropic particles comprising irregular compositions with immobilized transition metal particles have shown to be exciting heterogeneous catalysts<sup>1,2</sup>.

## 1.1 Catalysis

The Swedish chemist Jöns Jacob Berzelius introduced the term *catalysis* for the first time back in 1836<sup>3</sup>, derived from the Greek words *kata* (down) and *lyein* (loosen). Today catalysis is defined as “*the acceleration of chemical reactions by substances not consumed in the reactions themselves - substances known as catalysts*”, and a catalyst is defined as “*substances that accelerate chemical reactions without undergoing any net-reaction itself*”<sup>4</sup>. In order for a reaction to take place some requirements must be fulfilled regarding the molecules that react. As the reactants must come in contact, they must have or gain the energy to overcome the activation barrier (the activation energy) and they must also be correctly oriented relative to one another. A catalyst is said to lower the activation energy of the reaction by providing a different transition state, illustrated in **Figure 1.1** (exothermic reaction). As a result, catalysts can make reactions occur at lower temperatures and pressures and with increased reaction rates and selectivity. Therefore, catalytic processes are significant in the efforts to meet the demands and requirements of environmentally friendly processes in the industrial chemistry.

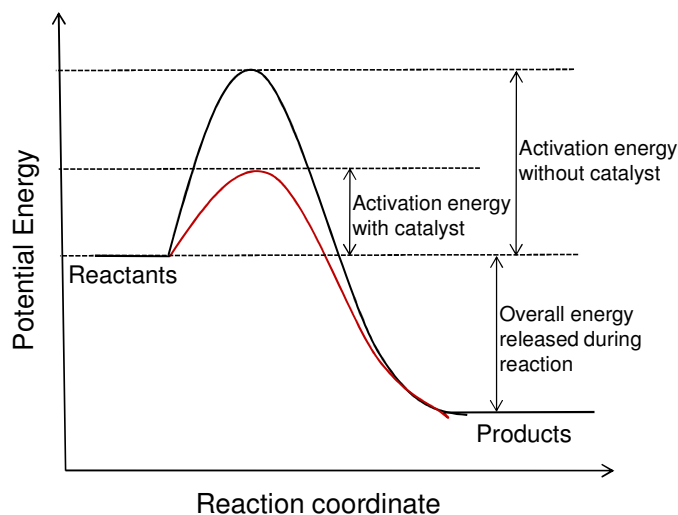


**Figure 1.1** Energy diagram of an exothermic chemical reaction illustrating the difference in activation energy between an uncatalyzed and a catalyzed reaction.

Catalysis can be divided into several groups depending on the nature of the operating catalyst of interest where some of them are biocatalysts, organocatalysts and transition metal catalysts. Biocatalysis involves enzymes as catalysts<sup>5</sup>, organocatalysis involves relatively small metal-free organic molecules as catalysts, whereas transition metal catalysis involves transition metals as catalysts. Depending on how the catalyst operate they can further be categorized into homogeneous- and heterogeneous catalysis. In heterogeneous catalysis the catalyst is defined to be in a phase different from the reagents and products whereas in homogeneous catalysis the catalyst is defined to be in the same phase as the reagents and products.

### 1.1.2 Transition Metal Catalysis

Transition metals are found in the middle block (or the d block) of the periodic table, e.g. in group 3-12, and they are said to be elements that are able to form stable ions with an incomplete filled d shell (orbital). Some of the transition metals show a number of useful properties as they can be colored, magnetic and catalytically active. Their usefulness in catalysis arises from their ability to adopt several different oxidation states and to form complexes allowing the metal to interact with a substrate in a

specific manner. One particular transition metal, namely palladium (Pd), has shown to exhibit excellent catalytic activity in a large number of reactions varying from oxidations and reductions to carbon-carbon bond formations<sup>6</sup>.

#### 1.1.2.1 Palladium Catalysis - Pd(II) Promoted Oxidations

The major breakthrough of Pd in catalysis is considered to be the development of the catalytic oxidation of olefins (alkenes) with palladium chloride (palladium(II)) to aldehydes and ketones, see **Figure 1.2a**, first reported back in 1959 and known to us as the Wacker-process<sup>7</sup>. This important industrial oxidation process started an era of Pd-catalyzed research which resulted in many versatile approaches. For example, Heck, Negishi and Suzuki developed the Pd(0) catalyzed cross-coupling reactions for organic synthesis<sup>8</sup>, see **Figure 1.2b**, resulting in the 2010 Nobel Prize in chemistry.

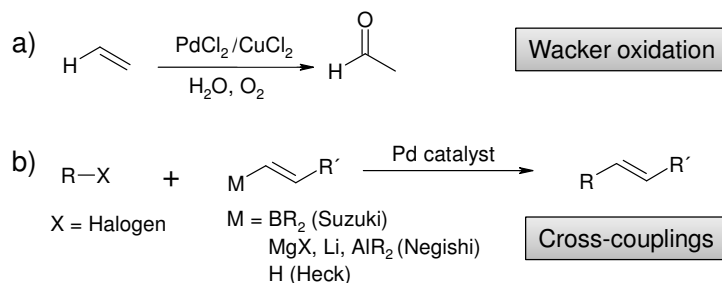


**Figure 1.2** Palladium-catalyzed chemical reactions. (a) Wacker oxidation of ethylene to acetaldehyde with palladiumchloride (Pd(II)) and (b) palladium(0)-catalyzed cross-coupling reactions developed by Heck, Negishi and Suzuki.

In the field of palladium(II)-catalyzed oxidations most of the developed methods such as Wacker-oxidations, aminations, and oxidative hetero- or carbocyclizations<sup>9</sup>, rely on alkene coordination to Pd(II), which makes the unsaturated hydrocarbon susceptible towards nucleophilic attack or migratory insertion resulting in an olefin derivatization or functionalization, see **Figure 1.3**. In addition to olefin derivatization approaches, Pd(II) has also extensively been used as catalyst in the selective oxidations of alcohols to ketones with molecular oxygen as terminal oxidant<sup>9</sup>.

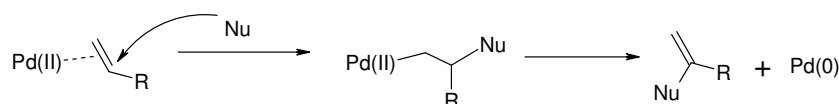


**Figure 1.3** Palladium(II)-catalyzed olefin derivatization. The double bond coordinates to Pd(II) making the alkene susceptible towards nucleophilic attack.

In a palladium(II)-catalyzed oxidation, Pd(II) is reduced to Pd(0). For the process to be catalytic it is necessary to re-oxidize Pd(0) back to Pd(II). In the Wacker process Pd(0) is re-oxidized to Pd(II) by Cu(II) under the formation of Cu(I), which in turn re-oxidized by molecular oxygen as terminal oxidant. Another way, among others, to re-oxidize Pd(0) is to use p-benzoquinone (BQ) as the oxidant, see **Figure 1.4** for a suggested pathway.

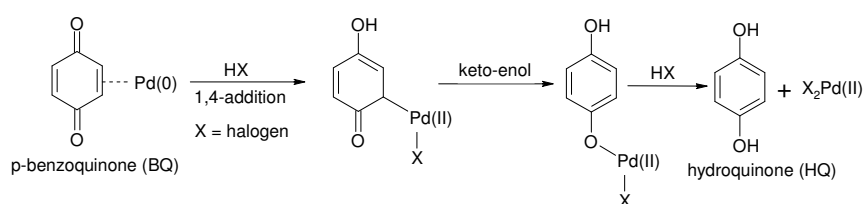


**Figure 1.4** Benzoquinone (BQ) promoted re-oxidation of palladium(0) to palladium(II) producing hydroquinone (HQ).

It is desirable to avoid the use of BQ and other organic- or metal based oxidants in stoichiometric amounts as the terminal oxidant to minimize the waste products and increasing the atomic efficiency of the process (*green chemistry*, see review article for the definition of green chemistry<sup>10</sup>). Therefore considerable effort has been addressed to find catalytic systems that allow the use of molecular oxygen as the terminal oxidant. In most cases the re-oxidation of Pd(0) to Pd(II) directly with molecular oxygen involves an moderately high activation barrier. Bäckvall *et al.*<sup>11</sup> developed a method where the Pd(0) re-oxidation where broken down into several steps, all involving low activation barriers, thus mimicking Nature's respiratory chain. This so called *biomimetic approach*<sup>12</sup> that relies on several coupled redox catalysts as electron transfer mediators (ETM's) has successfully been applied in several palladium(II)-catalyzed reactions ranging from carbocyclizations<sup>13</sup> to diene oxidations<sup>14</sup>. The biomimetic Pd(II) catalyzed aerobic oxidations are based on the use of an oxygen-activating transition metal complex (M(red)) which is directly oxidized (M(ox)) by molecular oxygen. The

latter can then oxidize HQ to BQ, which in turn can re-oxidize Pd(0) to Pd(II), see **Figure 1.5a**.

There are several transition metal ETM's capable of activating molecular oxygen including metal- phthalocyanines, salens, salophens and porphyrins<sup>15</sup>. Of particular importance to this thesis is the transition metal macrocycle *thioacetate-functionalized tetraphenyl cobalt porphyrin* and its ability to re-oxidize HQ to BQ with molecular oxygen, see **Figure 1.5b**.

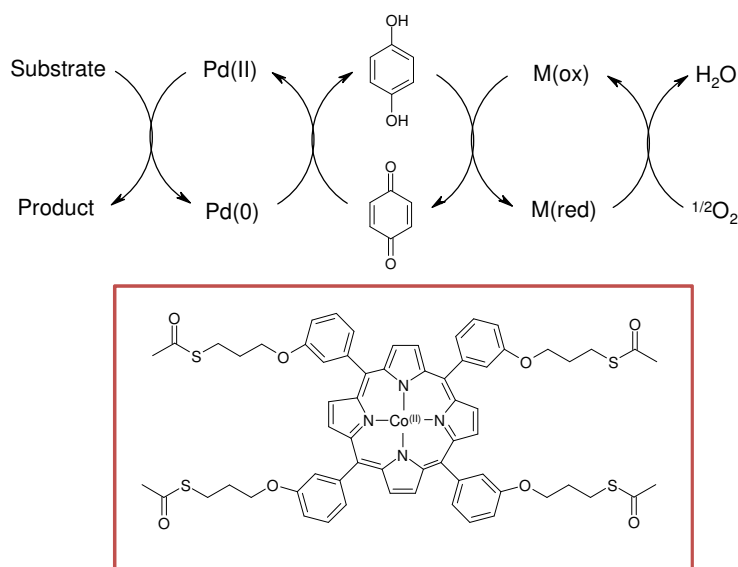


**Figure 1.5 (a)** Bäckvall's biomimetic approach involving several coupled redox catalysts as electron transfer mediators (ETM's) for Pd(II) catalyzed aerobic oxidations. **(b)** The transition metal macrocycle thioacetate-functionalized tetraphenyl cobalt porphyrin a candidate as an ETM in the biomimetic system.

### 1.1.3 Heterogeneous Catalysis

In heterogeneous catalysis the catalyst is not in the same phase as the reactants and products. The most common scenario is that the reactants are present in a gas- or liquid phase, whereas the catalyst is in the solid phase. The main advantage of having the catalyst in a separate phase is the *ease of separation* of the products from the catalyst.

This straightforward use of heterogeneous catalysts has made them interesting for industrial purposes for over a hundred years as Humphry

Davy in 1817 discovered that a preheated platinum wire became red hot upon exposure to air and coal gas and Johann Wolfgang Döbereiner during 1823 discovered that a fine jet of hydrogen catch fire when it was directed at a fine powered platinum<sup>16</sup>. The discoveries made by Davy and Döbereiner further resulted in some important innovations as the miner's safety lamp and the tinderbox (forerunner of the matchsticks), respectively, were developed and commercialized. Moreover, Paul Sabatier together with Senderens around 1900's facilitated the industrial use of hydrogenation as he discovered that trace amounts of finely divided nickel catalyses hydrogenation of unsaturated hydrocarbons<sup>17</sup>. Sabatier was further awarded the 1912 Nobel Prize in chemistry for his work on the metal-catalyzed alkene hydrogenations<sup>18</sup>.

Later on, perhaps the most important contribution of heterogeneous catalysis to mankind are the works made by Fritz Haber initiated in 1909 and further improved by Karl Bosch resulting in a method for the iron catalyzed conversion of hydrogen- and nitrogen gas into ammonia, known as the *Haber-Bosch process* for which they each obtained a Nobel Prize. In 1990 over 100 million tons of ammonia was synthesized worldwide<sup>16</sup>, which in large is responsible for the feeding of humans as the majority of the produced ammonia ends up as fertilizer in the agriculture. Furthermore, Karl Ziegler and Giulio Natta each contributed to the Ziegler-Natta catalyst for olefin polymerization which promoted the development of the entire plastic market.

#### *1.1.3.1 Mechanistic Understanding - Surface Confined Catalysis*

The mechanistic understanding of the surface-confined steps proceeding in a heterogeneous catalytic process have extensively been explored and explained by many researchers and among them Gerhard Ertl and Gabor Somorjai made significant contributions, which awarded Ertl the 2007 Nobel Prize in chemistry for his work on surface-confined chemical processes on solids. It is for instance due to Ertl that we now understand the different steps proceeding on the solid iron surface in the Haber-Bosch process<sup>19,20</sup>. A typical mechanism of a heterogeneous catalysis process on a solid transition metal catalyst, here represented by the catalytic oxidation of carbon monoxide to carbon dioxide on a platinum surface (e.g. auto-exhaust oxidation catalysis), is displayed in **Figure 1.6**. The mechanism, which is further extensively described in work by Ertl<sup>21,22</sup>, can be divided into several surface-confined reactions/actions or steps which all are taking place on the solid transition metal catalyst surface.

1. Adsorption of the reactants carbon monoxide (CO) and dioxygen ( $O_2$ ) from the gas phase on to the solid phase of the platinum surface.
2. Diffusion of the reactants on the platinum surface in order for CO and  $O_2$  to be correctly oriented to each other, providing molecular collisions.
3. Bond dissociation, the bonds between the oxygen atoms in the platinum surface adsorbed dioxygen are broken in order to form new bonds.  $O_2 \rightarrow 2O$
4. Bond formation (reaction), new bonds are formed between CO and O making  $CO_2$ .
5. Desorption of the reaction product  $CO_2$  from the solid platinum surface into the gas phase.  $CO_{2(ads)} \rightarrow CO_{2(g)}$

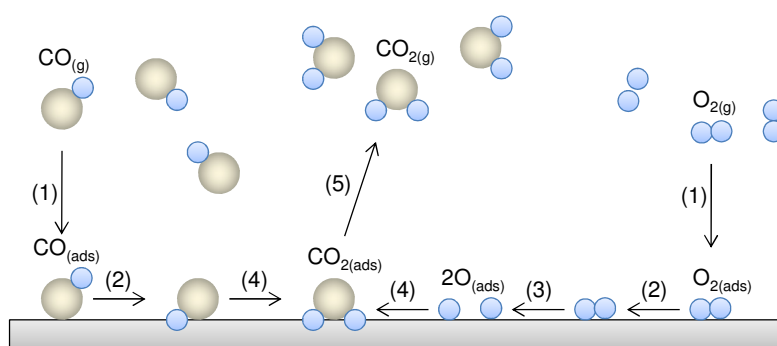


**Figure 1.6** Schematic illustration of the surface confined actions in the heterogeneous catalytic oxidation of carbon monoxide (CO) to carbon dioxide ( $CO_2$ ) with molecular oxygen on a platinum surface (the auto-exhaust oxidation catalysis). (1) adsorption of reactants on the catalyst surface (2) diffusion/migration (3) bond dissociation (4) bond formation (5) desorption of product from the solid catalyst surface.

The desorption of the reaction products from the catalyst surface is of particular importance since the adsorbed products hinder the adsorption of new reactants on to the catalyst surface and also the mobility of the adsorbed reactants thus inhibiting the catalytic turnover, a phenomena known as catalyst poisoning<sup>23</sup>. Addition of bonding modifiers to the catalyst surface have shown to influence the catalytic activity on transition metal surfaces. Both Ertl<sup>24</sup> and Somorjai<sup>25</sup> have shown that the desorption of produced ammonia on the iron surface in the Haber-Bosch

process can be facilitated by adding a small amount of potassium to the catalyst surface thus circumventing the problem with poisoning. The reason for this is that potassium weakens the bonding between ammonia and the iron surface by a repulsive donor-donor interaction thus decreasing ammonia's residence time on the catalyst surface and subsequently the turnover rate of nitrogen and hydrogen is uninhibited as it could be increased 30-fold<sup>25</sup>.

It has also been shown in a number of studies that the surface structure of the transition metal catalyst influences the turnover rates. Thus, Ertl<sup>26,27</sup> and Somorjai<sup>28,29</sup> demonstrated that surface defects on platinum surfaces, e.g. stepped-, kinked- or microstructured surfaces, increases the turnover rates in surface-confined reactions such as the oxidation of carbon monoxide and the dehydrogenation of cyclohexane, respectively.

Interfaces between transition metals and oxides are frequently considered to be essential in catalysis. These interface sites are thought to be anionic or cationic vacancies present at the edge of the metal oxide moieties<sup>30</sup>. Somorjai showed that the turnover rates of the hydrogenation of carbon monoxide to methane on rhodium surfaces decorated with oxides could be enhanced or retarded depending on the type of oxide used<sup>31</sup>, compared to an unpromoted rhodium surface. The activation of the C=O bond in carbon monoxide was proposed to occur via interaction of the oxygen with cationic vacancies at the metal-oxide interface sites thus activating the carbonyl group towards hydrogenation.

#### *1.1.3.2 Heterogenization of Homogeneous Catalysts*

The homogeneous catalysts are dissolved in the same phase as the reactants and products. Since transition metals work well under homogeneous conditions they have become one of the most important classes of homogeneous catalysts. Usually one or more organic ligands are coordinated to a transition metal making the complex to an organometallic catalyst. Generally, homogeneous catalysts contain a well defined *single active site*, regularly composed by the central transition metal surrounded by the ligands, while the heterogeneous catalysts usually contains a wide range of active sites. These well defined single active sites smoothes the progress of catalyst optimization making the homogeneous catalyst often more selective and specific compared to the solid catalysts.

The purpose of making a homogeneous catalytic process heterogeneous is to take advantage of the high selectivity of the homogeneous catalyst and the easy separation of the product from the catalyst of the heterogeneous system. This ease of separation *minimizes waste* derived from catalyst separation, allowing *recyclability* of the

catalyst (*green chemistry*<sup>10</sup>). From an economical standpoint, recyclability is of importance as the catalysts are sometimes the most expensive component in a catalytic process. Homogeneous catalysts are mostly heterogenized via attachment to solid supports either by physical adsorption or by covalent immobilization through chemical adsorption. Specific techniques for surface immobilization are presented in this thesis in the section on Surface Modification (see below). In some other examples the heterogenization is done by encapsulation of the catalyst in porous networks with the “ship-in-a-bottle” approach, for instance in zeolites<sup>32</sup>.

Since an enzyme often needs a transition metal in its active site in order to be active they consequently are to be considered as an important class of metal catalysts. In fact over 50 % of all known enzymes need a metal to be active<sup>33</sup>. The tertiary structure around the active sites of an enzyme is often arranged as a cavity, specifically designed to direct or reject reactants and coordinating ligands for the active transition metal complex. Enzymes are usually remarkable catalysts, developed and optimized by the nature itself during millions of years, performing reactions with excellent selectivity at relatively mild conditions. Although enzymes are known to be destabilized through surface interactions<sup>34</sup>, numerous successful enzyme immobilizations on solid surfaces have been utilized in penicillin- and aspartame synthesis, in lactose hydrolysis and in various biosensor applications<sup>35</sup>.

Metal macrocycles such as metal porphyrins are oxygen activating complexes that can be used as ETM's in Bäckvall's biomimetic approach for Pd(II)-catalyzed aerobic oxidation reactions, see section 1.1.2.1 on Pd(II) promoted oxidations. Some of these metal porphyrins are known to lose their activity under homogeneous conditions due to dimerization or other disabling self-oxidations processes<sup>36,37</sup>, resulting in an inhibition of the entire biomimetic system. One way to circumvent this problem is to immobilize the metal porphyrins on solid supports thus preventing the catalysts to interact with one another achieving an enhanced catalytic activity<sup>38,39</sup>. Berner *et al.* immobilized thioacetate-functionalized tetraphenyl cobalt porphyrins (CoTPP) on gold surfaces, see **Figure 1.7**, for investigation of catalyst orientation and activity<sup>40,41</sup>. They found that the heterogenized CoTPP molecules formed a complete monolayer on the gold surface at the same time as the activity in HQ oxidation could be increased 100-fold, compared to the homogeneous CoTPP. It was also found that the life-time of the catalyst was dramatically increased upon heterogenization as it displayed activity for over 300 hours.

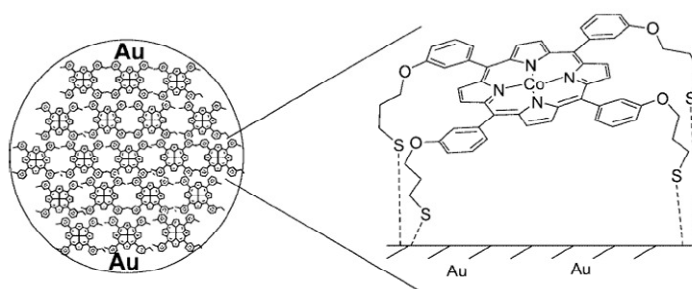


**Figure 1.7** Heterogenization of the homogeneous ETM thioacetate-functionalized tetraphenyl cobalt porphyrin (CoTPP) on gold surface via sulfur tails. Adapted with permission from *Eur. J. Org. Chem.*, **2006**, 1193. Copyright 2006 WILEY-VCH Verlag GmbH & Co. KGaA, Weinheim.

### 1.1.3.3 Transition Metal Nanoparticles - Semi Heterogeneous Catalysis

The use of transition metal nanoparticles in catalysis has increased dramatically in recent years.<sup>42</sup> As the metal nanoparticles are generally dispersed in the reaction solution as a homogeneous catalyst whereas the reaction is confined to its surface comprising several active sites as for a heterogeneous catalyst they are often categorized as semi heterogeneous catalysts, as the chemical process lies in the frontier between homogeneous- and heterogeneous catalysis. The transition metal nanoparticles are based on colloids or clusters containing from ten to several thousands of metal atoms varying in sizes from only one or a few nanometers to several hundreds of nanometers. The smaller of these metal nanoparticles e.g. from 25 to one nm (25 - 1 nm) have shown to be active in catalytic transformations with increasing activity when decreasing the size of the clusters, as the turnover rates for 2 nm particles could be about 8 times higher than for particles with a size of 12 nm<sup>43</sup>. Smaller particles have a higher percentage of surface atoms (larger surface-to-volume ratio) than larger particles consequently resulting in higher proportion of surface defects yielding more surface confined active sites, see **Figure 1.8**. As seen also for heterogeneous catalysts, semi heterogeneous mechanisms involving a variety of active catalytic sites are often more demanding to elucidate compared to single site mechanisms seen for the homogeneous catalysts.

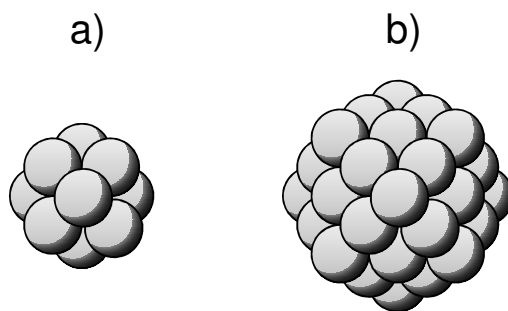


**Figure 1.8** Metal nanosized clusters; small nanoparticles (**a**) have a higher percentage of surface atoms than larger particles (**b**) resulting in higher proportion of surface defects yielding more surface confined active sites. Thus the small nanoparticles are more active than the larger particles.

One problem associated with metal nanoparticles is the lack of long-term stability due to the thermodynamically driven particle aggregation as small particles exhibit high surface energies due to the high percentage of surface atoms. When an aggregation to bigger clusters results in a minor percentage of surface atoms, the energy of the specific system of interest is lowered. One way to solve this problem is addition of surface-active ligands acting as stabilizers to the nanoparticles which has shown to increase the stability significantly<sup>44</sup>. Another way is to immobilize the metal nanoparticles on to solid supports, heterogenization. Also the immobilization of the semi heterogeneous catalyst on solid surfaces introduces reusability of the nanoparticles fulfilling the requirements of green chemistry. The metal nanoparticles are usually produced by chemical or electrochemical reduction of metal salts in presence of surface active ligands or solid supports in order to prevent the particle aggregation.

Gold nanoparticles (AuNP's) have extensively been used in recent years in various types of reactions as they have shown to exhibit some outstanding catalytic properties. It all started in 1984 when Hutchings discovered that gold ions catalyze the hydro-chlorination of acetylene<sup>45</sup>, until then gold was considered to be catalytically inactive. Some years later Haruta *et al.* showed that AuNP's heterogenized on transition metal oxides were active in carbon monoxide oxidation at low temperatures<sup>46</sup> and further on AuNP's alone were shown to catalyze alcohol oxidation in water<sup>47</sup>. Moreover, Hutchings and coworkers found that AuNPs on carbon with 25 nm dimensions were highly selective for aerobic oxidation of cyclohexene in different solutions at 80° C<sup>48</sup>. These findings started an era of AuNP catalyze research that can be considered as the

new gold rush<sup>49</sup>, see for instance review articles on Au and NP catalysis<sup>42,50</sup>. Heterogenized AuNP's have shown promising performance especially in oxidations of alcohols<sup>51,52</sup> and in hydrogenation reactions<sup>53,54</sup>, respectively.

Heterogenized palladium nanoparticles (PdNP's) have likewise been used in a variety of successful organic transformations such as oxidations<sup>55</sup>, hydrogenations<sup>56,57</sup> and carbon-carbon cross couplings<sup>58</sup>. Unlike as in the mononuclear homogeneous Pd(II)-catalyzed oxidation reactions, the palladium nanoparticles are able to directly activate molecular oxygen as a terminal oxidant allowing the use of PdNP's in aerobic oxidation reactions without the further use of ETM's as in the biomimetic approach, see section 1.1.2.1 on Pd(II)-Promoted Oxidations. Kaneda and co-workers<sup>55</sup> reported on a heterogenized Pd(II) catalyst for the efficient and selective aerobic alcohol oxidation. It was found that the actual catalytically active species was surface-confined PdNP's formed during the reaction. Although the complete mechanism for the aerobic oxidation reactions involving PdNP's is still unclear, palladium oxide (Pd(II)) is assumed to be the active species for the alcohol oxidation<sup>59</sup>. Kaneda's proposed mechanism for the aerobic alcohol oxidation with surface-confined PdNP's is displayed in **Figure 1.9**.

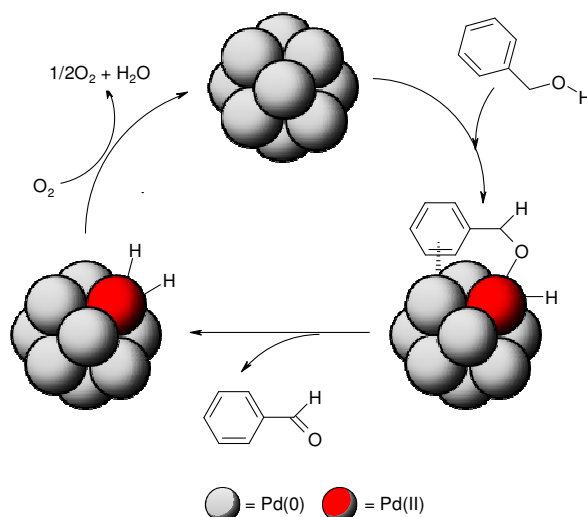


**Figure 1.9** Kaneda's proposed mechanism for the aerobic oxidation of alcohols with surface-confined palladium nanoparticles. The palladium nanoparticles are able to directly activate  $\text{O}_2$  as terminal oxidant allowing the use of the nanoparticles in aerobic oxidation reactions without the use of further ETM's as in the biomimetic approach for mononuclear homogeneous Pd(II) previously described.

## 1.2 Anisotropic Particles

During the last years there has been an increasing interest of going from isotropic- to anisotropic surfaces<sup>60</sup> in the area of surface chemistry. An isotropic surface means that the surface is uniform in functionality e.g. in terms of shape “morphology”, chemistry or magnetization. When it comes to anisotropic surfaces the surface instead possesses mixed (bi- or multifunctional) functionality. Casagrande *et al.*<sup>61</sup> and De Gennes<sup>62</sup> in 1992 introduced a new kind of material for surface anisotropy as particles comprising multi functionalities or compositions were for the first time described. Anisotropic particles can be divided in two categories; Patchy particles and Janus particles. Patchy particles can be considered as a particle with one or more patches thus exhibiting strong surface anisotropy, see **Figure 1.10a**. A Janus particle named after the Roman god Janus on the other hand can be defined as a particle with two faces or a particle with one patch which cover half of the particle surface, see **Figure 1.10b**. In recent years there has been an emerging interest regarding the preparation and applications of the anisotropic particles<sup>63</sup>.

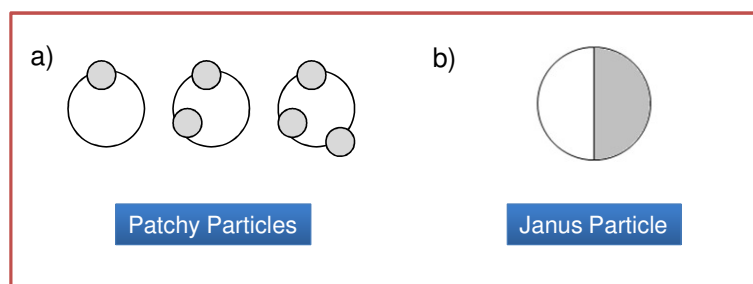


**Figure 1.10** Anisotropic particles, (a) Patchy particles with one, two and three patches, respectively, and (b) a Janus particle (two faces).

### 1.2.1 Preparation of Anisotropic Particles

There is a complete arsenal of different kinds of techniques utilized to prepare anisotropic particles and the methods can be summarized in three general approaches: phase separation, self-assembly, and masking<sup>64</sup>. This section will briefly describe some techniques that can be categorized in those three approaches.

The first approach, phase separation, explored by Feyen *et al.*<sup>65</sup>, is an approach based on seeded emulsion polymerization for the production of mushroom-like polystyrene-silica nanoparticles. Briefly the approach can be summarized in two steps, see **Figure 1.11**. Initially, magnetite ( $\text{Fe}_2\text{O}_3$ ) nanoparticles are partially encapsulated in polystyrene leaving a partially exposed iron oxide surface. Next, a silica shell is selectively grown over the exposed iron oxide producing the mushroom-like polystyrene-silica nanoparticle. The magnetite nanoparticle can be removed by hydrochloric acid treatment. Approaches based on microfluidics have also been used as a phase separation technique<sup>66,67</sup>, especially in attempts to scale up the production of anisotropic particles.

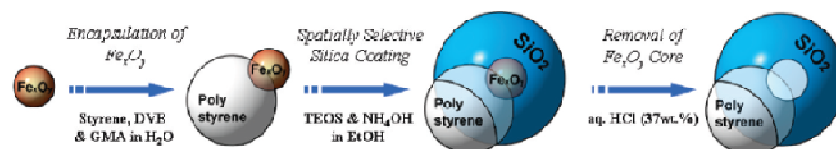


**Figure 1.11** Illustration of the phase separation procedure to prepare mushroom like anisotropic polystyrene-silica nanoparticles. Adapted with permission from *J. Am. Chem. Soc.* **2010**, 132, 6791.<sup>65</sup> Copyright 2010 American Chemical Society.

Secondly, the self-assembly approach has been extensively explored for the production of amphiphilic particles. An amphiphilic particle is a particle with one hydrophilic- and one hydrophobic face. Andala *et al.*<sup>68</sup> fabricated amphiphilic inorganic nanoparticles at the interface between two liquids, water and toluene. Inorganic nanoparticles present in this liquid interface exposes one face to water and the other to toluene. This makes half of the particle surface accessible for functionalization with a hydrophilic ligand and subsequently the other half accessible for hydrophobic functionalization thus generating the amphiphilic Janus particle, see **Figure 1.12**. Also the fabrication of non-spherical amphiphilic nanostructures like cylinders, ribbons and sheets via self-assembly has been demonstrated<sup>69</sup>.

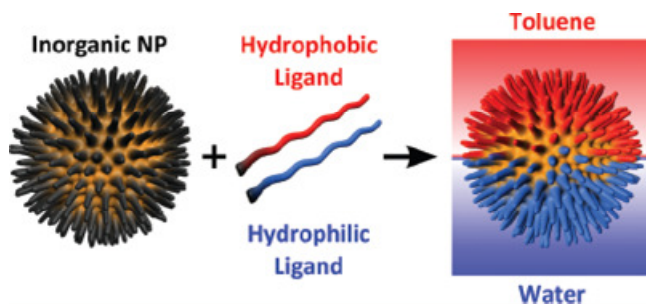


**Figure 1.12** Illustration of the formation of an amphiphilic Janus particle via self-assembly of a hydrophobic ligand from the toluene phase and self-assembly of a hydrophilic ligand from the water face. Adopted with permission from ACS Nano, **2012**, 6, 1044. <sup>68</sup> Copyright 2012 American Chemical Society.

The third method, the masking procedure, are based on the partial protection of the particle surface leaving the exposed part of the particles as an object for further functionalization while the protected part remains unchanged. The particles can be partially protected when adsorbing them on to flat substrates, on to larger particle surfaces or by micro contact printing. Cayre *et al.*<sup>70</sup> presented a micro contact printing method for the fabrication of asymmetrically coated colloidal particles, e.g. Janus particles. They used a polydimethylsiloxane (PDMS) stamp inked with a fluorescent molecule, a dye, and stamped a monolayer of 9.6  $\mu\text{m}$  sulphate latex particles on a glass slide. Janus-like (two phases) particles were obtained indicating that the dyes were successfully transferred only to the side of the particle that was in contact with the stamp leaving the protected part unchanged. See **Figure 1.13** for an illustration of the synthetic strategy to make Janus particles with micro contact printing.

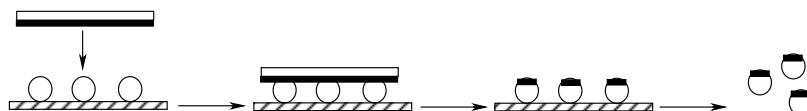


**Figure 1.13** Illustration of the strategy to produce Janus like particles with micro contact printing. The particles are partially protected when adsorbed on to a flat surface and the exposed part of the particle is further functionalized when it comes in contact with the stamp leaving the protected part unchanged thus generating a Janus particle.

### 1.2.2 Applications of Anisotropic Particles

Due to their asymmetric structure the anisotropic particles possess unique properties which make them interesting as tools in different applications. For instance, the amphiphilic Janus particles have been shown to be much more surface active than their corresponding isotropic particles<sup>71</sup> and spherical amphiphilic Janus particles have successfully been employed as surfactants in the emulsion polymerization of styrene<sup>72</sup>.

In drug delivery the application of anisotropic particles has been reported for the anticancer agent cisplatin. Upon hydrolysis the molecule is responsible for cell death and the non-specificity of this anticancer agent produces the destruction not only of tumors but also of healthy cells leading to undesirable side effects. Xu *et al.*<sup>73</sup> used Janus Au-Fe<sub>2</sub>O<sub>3</sub> nanoparticles for selective delivery of cisplatin only to breast cancer cells. The cancer cells possess often antigens overexpressed on their surface which can be used as targets for monoclonal antibodies. By binding the cisplatin complex to the Au surface and the antibodies targeting the cancer cell antigens to the iron oxide surface on the anisotropic particle the cisplatin drug was selectively delivered to the cancer cells leaving the healthy cells unharmed.

Another exciting approach for anisotropic particles is the application in multiplex diagnostics<sup>74</sup>. A multiplex diagnostic is an assay where multiple interactions are analyzed in a single sample volume. Each type of anisotropic particle has a specific code, often a color combination<sup>75</sup> see **Figure 1.14a**, which is used to identify the particle and subsequently also the interaction that the particle is coupled to. The multi-functionality of anisotropic particles compared to isotropic particles enables the design of a larger variety of barcodes on the particles thus enabling the possibility to identify much more interactions in a single sample volume which often decreases the time-costs for the analysis. This approach to employ barcodes on particles shows potential in clinical diagnostics and drug discovery for studies of protein, DNA, drug, receptor and antibody-antigen interactions.

#### 1.2.2.1 Anisotropic Particles in Heterogeneous Catalysis

In the field of catalysis, some interesting activities of anisotropic particles mainly with the patchy-like structures involving metal nanoparticles immobilized on metal-oxide particles or vice versa, so called particles-on-particle morphology, have previously been reported<sup>60</sup>. These asymmetrical particles possess the catalytically interesting transition metal-metal oxide interfaces previously described, see section 1.1.3.1 on

mechanistic understanding - surface confined catalysis. Au-Fe<sub>2</sub>O<sub>3</sub> and Pt-Fe<sub>2</sub>O<sub>3</sub> patchy particles have successfully been used in carbon monoxide oxidation where the activities at low temperatures were found to be higher than for the commercial catalysts.<sup>76</sup> She *et al.* reported recently on the use of patchy-like Au-TiO<sub>2</sub> particles as photocatalysts under visible light irradiation for the production of hydrogen (H<sub>2</sub>) from a solution of isopropyl alcohol and water<sup>1</sup>, see **Figure 1.14b**. The generation of H<sub>2</sub> was largely increased when using the asymmetrical Janus particles compared to the use of bare gold nanoparticles and amorphous TiO<sub>2</sub>. The Janus Au-TiO<sub>2</sub> particles showed even higher photocatalytic activity than core-shell TiO<sub>2</sub>-Au particles indicating a synergistic effect between the components in the asymmetric structure.

Further, the catalytic activity of Janus particles has also been utilized to design so called nanoengines<sup>2</sup>. Nanoengines are nanoparticles that employ a chemical reaction to obtain a certain self-propulsion to overcome the Brownian motion.

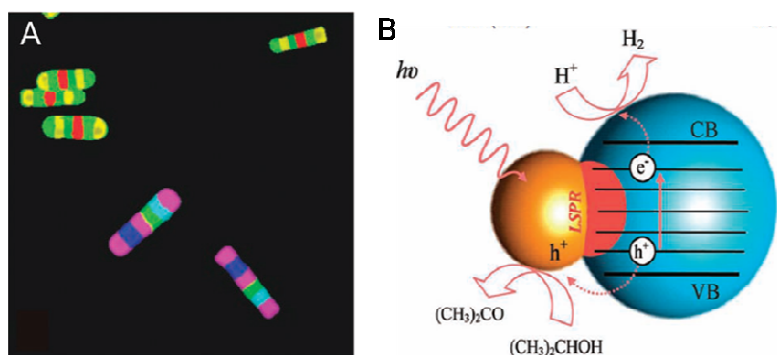


**Figure 1.14** Application of anisotropic particles. (A) Fluorescence microscopy images of color coded anisotropic particles. Adapted from *Proc. Natl. Acad. Sci. U. S. A.*, **2003**, 2, 389. (B) Proposed photocatalytic process for the generation of hydrogen (H<sub>2</sub>) using Janus Au-TiO<sub>2</sub> nanoparticles. The H<sub>2</sub> generation was largely increased when using the asymmetrical Janus particles compared to the use of bare gold nanoparticles, amorphous TiO<sub>2</sub> and than core-shell TiO<sub>2</sub>-Au particles. Adapted from *Adv. Mater.*, **2012**, 24, 2310. Request sent

## 2. Methods

### *2.1 Surface Modifications used in the Thesis*

In most surface modification techniques a compound is attached that differs chemically or physically from the surface thus introducing a new functionality. The compound molecules are bound to the surface either through physical adsorption (physisorption) or chemical adsorption (chemisorption). Physical adsorption is generated via bonds consisting of van der Waals type forces depending on the molecules involved whereas chemical adsorption is stronger bonds with covalent character. Common surface modification techniques are photolithography and micro contact printing that utilizes physisorption and chemisorption, respectively<sup>77</sup>. This chapter will go through surface modification techniques that have been used in this thesis.

#### *2.1.1 Introduction of Thiols on Silicon Surfaces in Paper I, III and IV*

In order to couple ligands or introduce certain functionality onto substrate surfaces such as silicon<sup>78,79</sup>, silica<sup>80,81</sup> and metal oxides<sup>82,83</sup> silanization is often used. A common features of these substrates is the surface hydroxyl groups (-OH) which are reactive towards the alkoxysilanes. When surface silanol groups (Si-OH) on silicon react with the alkoxysilanes (Si-O-CH<sub>3</sub>/C<sub>2</sub>H<sub>5</sub>) they displace the alkoxy groups and thus forming -Si-O-Si-bonds. Hence the silane molecules are covalently attached to the silicon. In order to introduce thiols (-SH) on silicon *e.g.* (3-mercaptopropyl) methyl dimethoxy silane (MPMDMS) are reacted with the silanols on the silicon surface, see **Figure 2.1**. Amino groups are often introduced on silicon or silica surfaces in this manner by the use of amino- instead of mercaptosilanes.

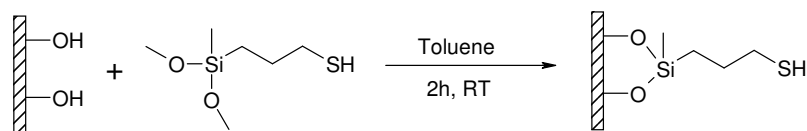


**Figure 2.1** Introduction of thiols on a silicon surface by reacting the silanol groups with (3 -mercaptopropyl) methyl dimethoxy silane (MPMDMS) in toluene for 2 hours at room temperature.

### 2.1.2 Introduction of Thiols on Amino-Functionalized Surfaces in Paper II, III and IV

Primary amines ( $\text{-NH}_2$ ) can be modified with thiols by coupling N - succinimidyl 3 - (2-pyridyldithio) - propionate (SPDP) with the amino groups thus introducing SS-pyridyl groups, see **Figure 2.2a**. By reducing the SS-Pyridyls with dithiothreitol (DTT) as described by Cleland<sup>84</sup> the disulphide bond ( $\text{-SS-}$ ) is cleaved forming the free thiols ( $\text{-SH}$ ), see **Figure 2.2b**. The SPDP molecule was first developed by Carlsson *et al.*<sup>85</sup> as a bioconjugate reagent for reversible cross-coupling of proteins at physiological conditions. The two proteins to be cross-coupled are first reacted with SPDP for introduction of the SS-pyridyl groups.

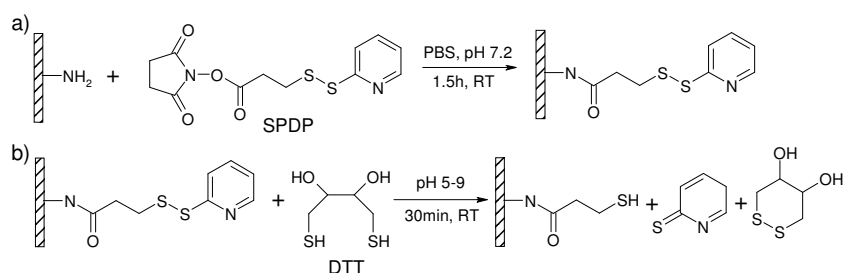


**Figure 2.2** Thiolation of amino-terminated surfaces. The surface bound primary amines were reacted with N -Succinimidyl 3 - (2-pyridyldithio) - propionate (SPDP) in phosphate buffered saline (PBS) for 1.5 hours at room temperature to introduce SS-pyridyl groups (a) which afterwards can be reduced with dithiothreitol (DTT) in a water solution pH 5-9 for 30 minutes to yield thiols (b).

One of the two proteins is then reduced with DTT thus forming free thiols on that protein as described above. Now the two proteins can be coupled by reaction of the free thiols with the SS-pyridyl groups forming stable disulphide bonds between the proteins, see **Figure 2.3a**. The

disulphide bond holding the proteins together can subsequently be reduced by reaction with DTT, see **Figure 2.3b**, making a release of the two cross-coupled proteins. The method is not only restricted to proteins as it is widely used for coupling of almost any kind of ligands that possess primary amines or thiols. In Paper I and II this reaction was used to immobilize thiol-functionalized tetraphenyl cobalt porphyrins on SS-pyridyl-modified silicon wafers and silica particles.

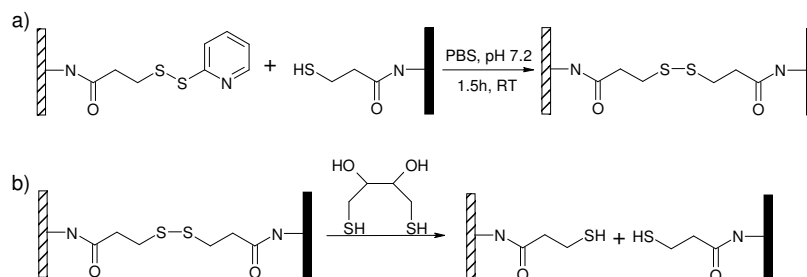


**Figure 2.3** Reversible cross-coupling of proteins at physiological conditions. (a) SS-pyridyl modified protein is reacted with thiolated protein in order to couple the proteins via disulphide bonds (S-S). (b) Release of the proteins by reduction of the disulphide bonds with DTT.

### 2.1.3 Determination of the Thiol Concentration in Paper II, III, IV and V

The concentration of thiols can be spectrophotometrically determined by reaction of the free thiols with 2,2'-dipyridyl-disulphide (2PDS), see **Figure 2.4**, at physiological conditions as first described by Brocklehurst *et al.*<sup>86</sup>. The concentration of the product pyridin-2-thione in the reaction solution can be calculated by determining the absorbance at wavelength 343 nm since it has a molar extinction coefficient of 8080 M<sup>-1</sup>cm<sup>-1</sup> and one free pyridin-2-thione correlates to one thiol molecule. Pyridin-2-thione is also produced when DTT reduces SS-pyridyls, see **Figure 2.2b**, thus the generated free thiols can be calculated.

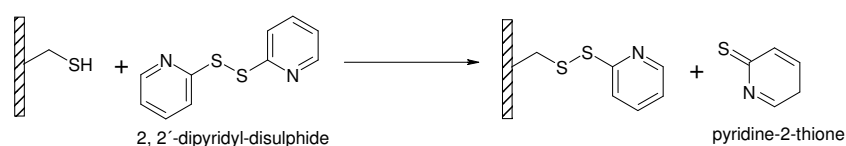


**Figure 2.4** Reactions of thiol with 2, 2'-dipyridyl-disulphide in order to analyze the concentration of thiols by determine the absorbance at the wavelength 343 nm of pyridine-2-thione.

#### 2.1.4 Immobilization on Gold Through the Sulfur-Gold Interaction in Paper IV and V

Sulfur-containing molecules such as organosulfurs (-RS) like alkyl-disulfides<sup>87</sup>, thioethers<sup>88</sup>, xanthates<sup>89</sup> and thiocarabamates<sup>90</sup> and thiols, see **Figure 2.5a**, are known to have a strong affinity to gold atoms. The most studied and perhaps most understood among these organosulfurs are the adsorption of alkanethiols or alkanethiolates (-RSH) on gold surfaces which are frequently used for the formation of Self Assembled Monolayers (SAMs). However, the first report regarding organosulfur-SAMs on gold surfaces from 1983 considered instead alkyldisulfides<sup>87</sup>. In the reaction, alkanethiol is adsorbed to the gold surface followed by a displacement of the hydrogen (-H), deprotonation of -RSH, thus forming a thiolate-gold complex ( $\text{-RS}^{-1}\text{-Au(I)}$ ), see **Figure 2.5b**. In the interaction with the alkanethiol and gold, the thiolate ( $\text{-RS}^{-1}$ ) molecule has been characterized as the adsorbing specie with techniques like X-ray Photoelectron spectroscopy (XPS)<sup>91</sup>, Raman spectroscopy<sup>92</sup> and electrochemistry<sup>93</sup>. The bond between  $\text{-RS}^{-1}$  and Au(I) is categorized as a strong semicovalent bond with a bond strength of approximately 40 kcal/mol<sup>94</sup>. Furthermore, organosulfurs also show strong affinity to other type of metals such as mercury<sup>95</sup>, silver<sup>96</sup>, copper<sup>91</sup>, platina<sup>97</sup> and iron<sup>98</sup>. This spontaneous bond formation between thiol and gold is commonly employed in various applications. Among many, as *e.g.* in electrochemistry the interaction is used to immobilize thiol-ligands on gold electrodes in order to produce modified electrodes<sup>99</sup>. The affinity also enables the formation of nano-sized air- and thermally stable gold particles first reported in 1994 by Brust and Schiffrin<sup>100</sup>. In this report the thiol-gold interaction protected the gold nanoparticles formed to agglomerate thus preventing the generation of bigger particles, so called thiol-protected gold nanoparticles.

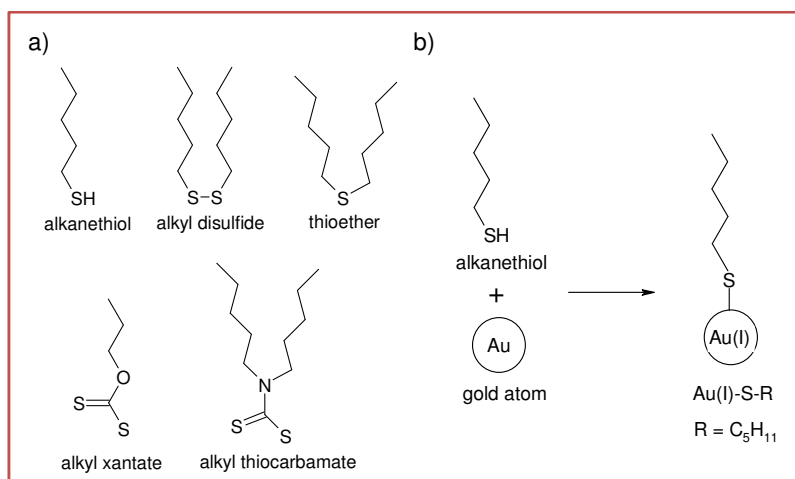


**Figure 2.5** The gold to sulfur interaction. (a) Illustrates some organosulfurs that shows strong affinity to gold atoms. (b) The reaction between the alkanethiol (-SH) and gold (Au) producing the stable Au(I)-S<sup>-</sup> semi covalent bond.

## 2.2 Electrochemistry - Principle and Definitions

Electrochemistry is the branch of chemistry concerned with the interrelation of electrical and chemical effects<sup>101</sup> and the interconversion of chemical- and electrical energy. Principally, with electrochemistry reactions are studied at the interface between an electronic conductor (*electrode*), typically composed of metal or carbon, and an ionic conductor (*electrolyte*), which involve electron (*charge*) transfer across between the electrode and the electrolyte. Further, the charge is carried through the electrode by the movements of electrons while in the electrolyte it is transported by the movements of ions. There are two main types of electrochemical cells where the interconversion of the electrical and chemical energy takes place. In an *electrolytic cell* one applies a potential difference between the electrodes in order to induce redox reactions whereas in a *galvanic cell*, as a battery, one uses spontaneous redox reactions in order to gain electrical energy. A *redox* reaction is a paired *oxidation/reduction* where one species is oxidized when the other one is reduced. In general, the electrochemical cell consists of two electrodes, the *anode* and the *cathode*. The anode is the electrode where the oxidation takes place, leading to a release of electrons, whereas the cathode is where the reduction involving a consumption of electrons

occurs. Commonly in electrochemistry the oxidation- and reduction reactions are separated from each other in space by the electrolyte, but connected through an external electrical circuit which transports the electrons from the anode to the cathode, see **Figure 2.6**.

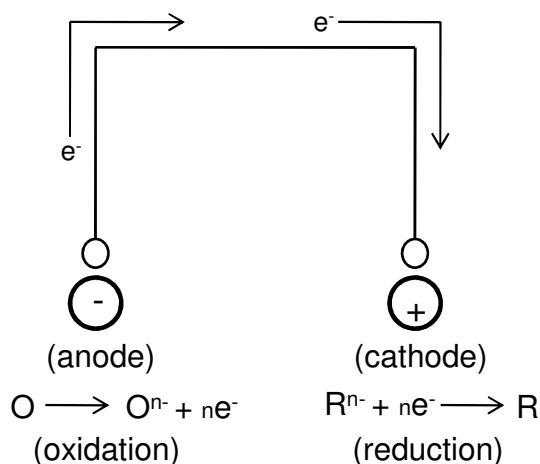


**Figure 2.6** Illustration of an electrochemical cell where the oxidation reaction generates electrons at the anode electrode which then are transported via the external electrical circuit to the cathode electrode where the electrons are consumed in a reduction.

In general, one is only interested in reactions that occur at either the anode- or the cathode. In such cases the electrochemical cell could be considered as composed of two half cells with the electrode system of interest, the working electrode, and a reference electrode. A reference electrode is assumed to have a constant or fixed potential due to its constant composition making any observed change in the electrochemical cell potential ascribable to changes in the working electrode potential. By connecting the electrochemical cell to a power supply one can force the working electrode to operate as an anode or cathode. By applying more positive potentials to the working electrode with respect to the reference electrode an increasing *oxidation current* will be seen at the working electrode. Analogously, by applying a more negative potential to the working electrode with respect to the reference electrode an electron flow in the opposite direction, will be obtained, resulting in an increased *reduction current* at the working electrode.

An electrochemical cell composed of a working electrode and a reference electrode is called a *two-electrode setup* whereas a cell comprising a working electrode, a reference electrode and an *auxiliary*

(counter) electrode is called a *three-electrode setup*. The additional auxiliary electrode is used to ensure that the passage of current through the reference electrode does not affect its potential, which subsequently results in that the observed changes in the cell potential cannot be ascribed only to changes in the working electrode potential. In the three-electrode setup, the current is instead passed between the working and auxiliary electrode while the potential of the working electrode is measured versus the reference electrode.

### 2.2.1 Electrochemical Oxidation of Surface-Confined Thiols in Paper III

In 1991 Batista-Viera *et al.*<sup>102</sup> reported on a method for reversible immobilization of thiol-containing biomolecules, e.g. thiol-containing peptides and proteins, on an agarose gel. They oxidized agarose coupled thiols to yield reactive thiolsulfonates ( $-\text{SO}_2$ ) using hydrogen peroxide ( $\text{H}_2\text{O}_2$ ) as an oxidant. The  $-\text{SO}_2$  functional groups showed strong reactivity towards  $-\text{SH}$  groups as they quickly formed disulfide bonds with the thiols. The  $-\text{SO}_2$  activated agarose could therefore be successfully coupled to the thiol-containing peptides which subsequently also were released by DTT cleavage similar, in accordance with the description in section 2.1.1.2, **Figure 3b**.

In 2003 Pavlovic *et al.*<sup>103</sup> used a two-electrode electrochemical approach to oxidize surface-confined thiols, where a conductive silicon surface with immobilized  $-\text{SH}$  groups was used as a working electrode coupled to a platinum electrode in a PBS buffer solution acting as the electrolyte. By applying more positive potentials to the working electrode with respect to the combined platinum reference and counter electrode, the authors were able to oxidize the surface-bound thiols as the silicon electrode served as the anode. The electrochemical oxidized products were characterized with X-ray Photoelectron Spectroscopy (XPS) to contain both thiolsulfinates and thiolsulfonates. These reactive structures were further used to immobilize thiol-biomolecules onto the silicon surface.

Further, the authors were able to produce micrometer patterns of thiol-biomolecules or thiol-particles on the conductive thiolated silicon surface by utilizing a patterned aluminum stamp as a combined reference- and auxiliary electrode<sup>104</sup>, see **Figure 2.7**. When the stamp was brought in contact with the thiolated silicon surface and a positive potential was applied to the silicon surface, the thiols closest the aluminum stamp were electrochemically oxidized, leaving the thiols situated furthest from the combined auxiliary/reference electrode un-oxidized. The generated

anisotropic silicon surface, with respect to the surface-confined thiols and reactive thiolsulfonates/thiolsulfonates, where further functionalized in order to produce micron sized patterns of thiol-biomolecules and thiol-particles.

Moreover, the authors also used an Atomic Force Microscopy (AFM) tip as a reference electrode, instead of the patterned aluminium stamp, in order to electrochemically generate patterns of thiol-biomolecules on to the conductive thiolated silicon surface on the nanometer scale<sup>105</sup>. This presented approach, electrochemical microcontact printing or electro-micro contact printing, is an alternative method to more traditional methods, e.g. photolithography and micro contact printing, for site-specific immobilizations on flat surfaces.

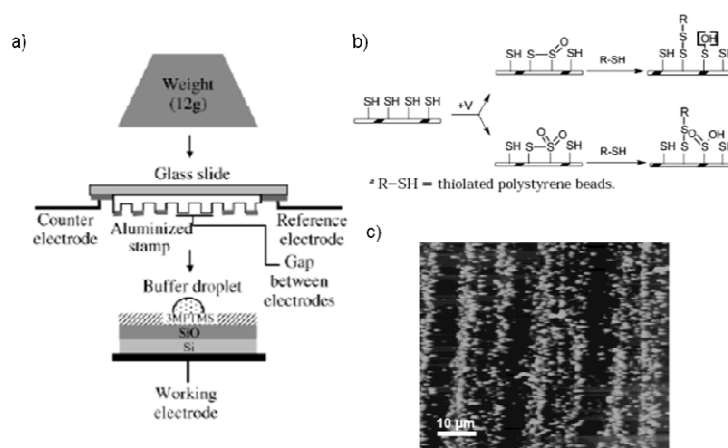


**Figure 2.7** Electrochemical generation of thiol-reactive patterns on flat surfaces. (a) The electrochemical microcontact printing setup. (b) A potential of +0.65 V (versus Ag/AgCl) oxidizes the thiols to reactive thiolsulfonates and thiolsulfonates. Thiolated polystyrene beads are covalently attached through formation of disulfide bonds with the electro-activated surface. (c) Tapping mode AFM image of thiolated polystyrene beads immobilized to electro-activated patterns on a silicon surface. The linear patterns correspond to the patterned aluminum stamp used in the electrochemical printing step. Adapted with permission from *Langmuir*, **2003**, 19, 10267.<sup>104</sup> Copyright 2003 American Chemical Society

### 3. Thesis Aim and Objectives

This thesis focuses on developing surface-confined transition metal complexes for application in heterogeneous catalysis and for the preparation of anisotropic particle surfaces. In previous work by our group the homogeneous transition metal macrocycle catalyst tetraphenyl cobalt porphyrin was heterogenized on gold surfaces with a 100 times boosted activity compared to the homogeneous congener. Therefore this thesis starts with the heterogenization of the same catalyst on silicon wafers and on silica particles for further up-scaling purposes as particles offers superior surface area at the same time as the volume can be reduced, Chapter 4.

Previously our group developed a method based on electrochemical oxidation of thiols for the site-specific heterogenization of thiol-proteins and thiol-particles for preparation of flat anisotropic surfaces. In Chapter 5 and 6 we explore the possibilities to manufacture anisotropic spherical particle surfaces with electrochemistry as surface-confined patches or gold gradients were formed on the particles. The surface-confined gold species were further evaluated as heterogeneous catalysts in the cycloisomerizations of 4-alkynoic acids to lactones.

Finally in Chapter 7, the synthesis and characterization of heterogeneous palladium nanoparticles on mesocellular foam are described together with its activity and recyclability in the aerobic oxidation of primary and secondary alcohols.

## 4. Performance of a Biomimetic Oxidation Catalyst Immobilized on Silicon Wafers and Silica Particles: Comparison with Its Gold Congener (Paper I and II)

### 4.1 Introduction

The oxygen-activating metal porphyrins are used as electron transfer mediators (ETM's) in biomimetic approaches for Pd(II)-catalyzed aerobic oxidations introduced by Bäckvall *et al.*<sup>15</sup>. One drawback of using the metal porphyrins is that they exhibit low stability due to dimerization under homogeneous conditions<sup>38,39</sup>. This problem was solved by immobilization of the catalyst tetraphenyl cobalt porphyrin (CoTPP) using gold wafers as support which allowed a rather straightforward immobilization of a CoTPP functionalized with thioacetates<sup>40</sup> and attached through gold-sulfur bonds, see **Figure 1.7**. Utilizing a flat surface as support for the catalyst allowed the use of surface-characterizing techniques such as Scanning Tunneling Microscopy (STM) and Atomic Force Microscopy (AFM) to investigate the orientation of individual catalyst molecules on the surface. The catalyst activity was evaluated by following the oxidation of hydroquinone (HQ) to p-benzoquinone (BQ), an important step in the biomimetic approach where BQ in turn reoxidizes Pd(II), see **Figure 4.1**. It was found that the CoTPP molecules formed a complete monolayer on the gold surface whereas the activity was increased 100-fold as it was maintained for over 300 hours. The homogeneous CoTPP was deactivated already after a few hours<sup>41</sup>.

Based on these findings we wanted to extend these studies using silicon wafers (paper **I**) and silica particles (paper **II**) as supports for the catalyst heterogenization to see if this dramatic boost upon immobilization is maintained on other support surfaces and also to evaluate eventually synergistic effects between the gold and CoTPP. A Si wafer were chosen as support since it is cheaper than gold, it is widely used and accepted in many fields, it shows more material flexibility, and it also allows the use of surface-characterizing techniques, as for other

flat surfaces, to determine the catalyst organization on the support surface. Silica particles on the other hand increase dramatically the active surface area at the same time as the volume can be reduced, which remove limitations for scale-up processes associated with flat support surfaces. Both silica- and magnetic silica were evaluated as particle supports where the magnetization allows easy separation and recyclability of the catalyst by use of permanent magnets. Silicon wafer and silica particle surfaces on the other hand did not allow the same straightforward attachment approach as gold surfaces since both supports and catalyst need additional activation for the immobilization. These extra activation steps were shown to be of importance for the orientation and organization of the catalyst and subsequently also essential for the catalyst's activity.

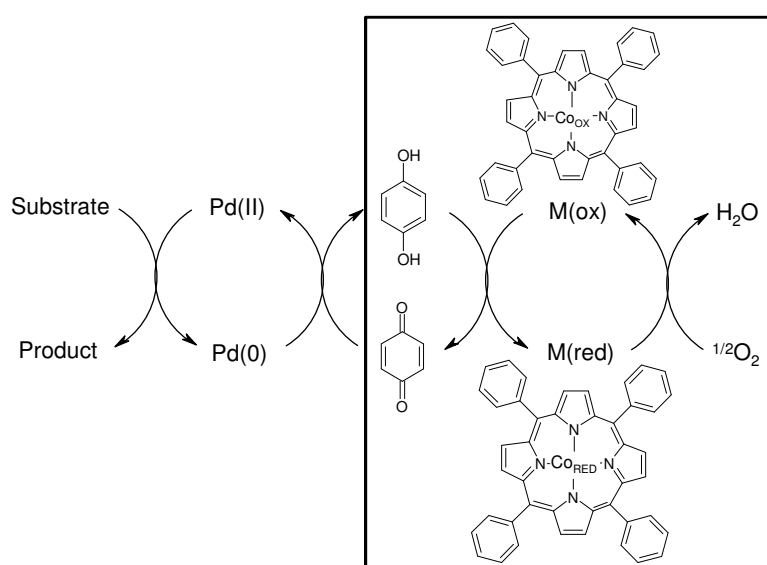


**Figure 4.1** Oxidation of hydroquinone (HQ) to benzoquinone (BQ) by the ETM cobalt tetraphenyl porphyrin with molecular oxygen as terminal oxidant. Oxidation of HQ is an important step in the biomimetic approach.

## 4.2 Results and Discussion

### 4.2.1 Heterogenization of the Catalyst

The homogeneous catalyst tetraphenyl cobalt porphyrin (CoTPP) was functionalized with thiol “legs” in the form of thioacetate groups<sup>40</sup> in order to prevent intermolecular dimerization by forming disulfides. Thioacetates can easily be converted to thiols by treatment with base or acid thus allowing immobilization on support surfaces by the means of thiol / SS-pyridyl exchange, see section 2.1.2 and **Figure 2.3a**. Therefore the Si wafer and silica particle surfaces were modified with SS-pyridyl groups prior to the catalyst’s heterogenization.

The Si wafers were modified with SS-pyridyl groups by initially react the silanol groups with mercaptosilane thus forming thiols and disulfides. The disulfides are formed between thiols in close contacts. The silanization was followed by reaction with both pyridin-2-thione and 2, 2'-dipyridyl-disulphide (2PDS) to be able to get all the thiols and disulfides reactive and stabilized. The thiol-functionalized CoTPPs were subsequently heterogenized on to the SS-pyridyl activated Si wafers. The silica particles were reacted with SPDP in order to introduce the surface-confined SS-pyridyl groups as the particles possessed primary amines. The thiol-functionalized CoTPPs were then immobilized through a thiol-disulphide exchange reaction. For an overview of the different steps utilized to immobilize the thioacetate-functionalized CoTPPs on the Si wafers and silica particles see **Figure 4.2**.

The loadings of CoTPP on the silicon wafers, silica particles, and magnetic silica particles were determined with Inductively Coupled Plasma - Mass Spectrometry (ICP-MS) by analysis of cobalt (Co). On the silicon wafers the cobalt loading was found to be around 20 nmol per 150 cm<sup>2</sup> wafer (130 pmol/cm<sup>2</sup>) whereas the cobalt loadings on the silica- and magnetic silica particles were found to be about 4 nmol per 100 mg particles (42 ppm, w/w) and 9 nmol per 100 mg particles (98 ppm, w/w), respectively, corresponding to 2 pmol/cm<sup>2</sup> and 4.5 pmol/cm<sup>2</sup>, respectively.

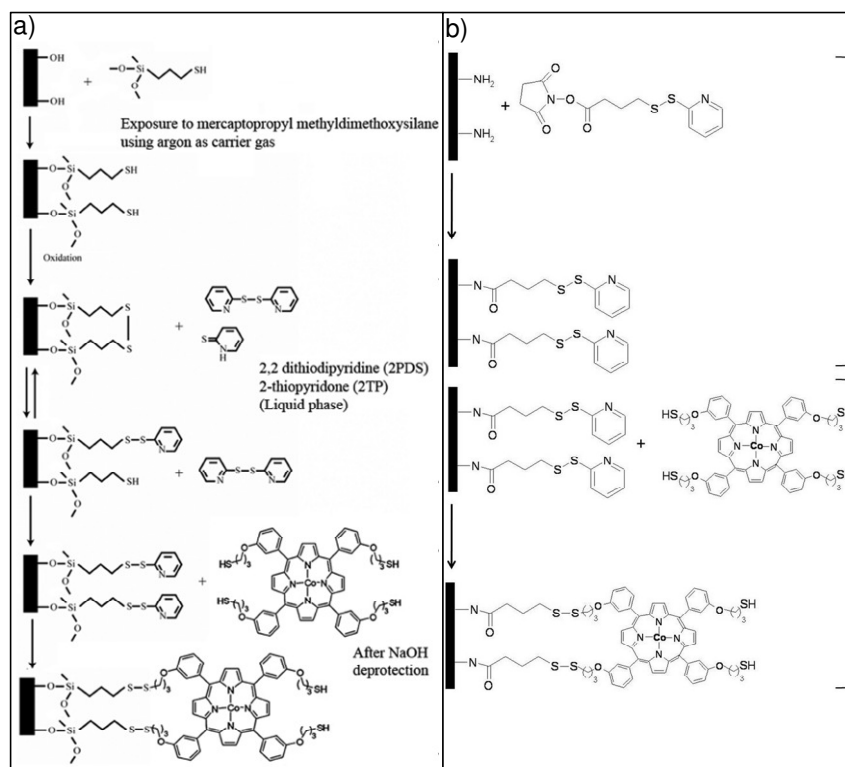


**Figure 4.2** Schematic figure of the different surface modification steps in order to heterogenize the thiol-functionalized cobalt porphyrins on **(a)** silicon wafers and **(b)** silica particles. The deprotection step of the catalyst thioacetate-legs to thiol-legs with base is not displayed in the figure. Prior to catalyst immobilization the support surfaces are activated by modification with SS-Pyridyl groups.

## 4.2.2 Organization of the Heterogenized Catalysts

### 4.2.2.1 Atomic Force Microscopy Study

One of the prospects of using an ultraflat silicon wafer as one of the supports for catalyst heterogenization was that it allows the use of surface-characterizing techniques to evaluate how the catalyst molecules were organized on the support surface and for this mission Atomic Force

Microscopy (AFM) was used. In **Figure 4.3**, AFM images of the SS-Pyridyl activated silicon surface prior (a) and after (b) attachment of the thiol-functionalized CoTPPs together with an image of the surface taken after it was employed in the reoxidation reaction of BQ (c) are displayed. As seen in the image after CoTPP attachment, clusters in sizes of 30-50 nm in height and 100-200 nm in width are present on the Si wafer surface, clusters that are absent prior to the attachment indicating formation of CoTPP complexes as clusters and multilayers. During the deprotection step of the thioacetate “legs”, e.g. formation of free thiol-linkers, aggregates of molecules were detected in the solution. Since it was absent in the solution prior to NaOH addition their formation is thought to be attributed to a base-promoted disulfide formation<sup>106</sup> between CoTPPs thus generating the clusters and multilayers seen on the silicon wafer surface. The AFM image recorded on the silicon wafer after utilization in the BQ reoxidation reaction indicates reorganization of the layers of surface-confined CoTPP catalysts as the clusters seem to decrease in quantity and size.

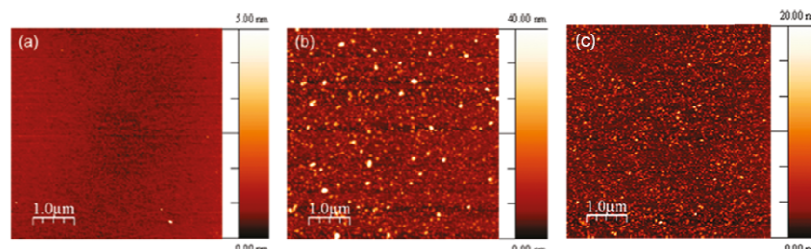


**Figure 4.3** Atomic Force Microscopy (AFM) images acquired on SS-Pyridyl activated silicon wafer surfaces prior (a) and after (b) attachment of the thiol-functionalized CoTPPs and after (c) utilization in the reoxidation reaction of BQ.

#### 4.2.2.2 X-ray Photoelectron Spectroscopy Study

Evaluation of the organization of the CoTPP on the particle surfaces with AFM is not as straightforward as it is on an ultraflat surface. In order to gain some information about the orientation and organization of the immobilized CoTPP molecules on the silica particles we used X-ray Photoelectron Spectroscopy (XPS) to see if some information could be gained from the oxidation states of the surface-confined Co by comparing the binding energy values obtained on the gold surfaces, silicon wafers and silica particles.

The binding energy (BE) values of Co2p<sub>3/2</sub> from the different support surfaces are displayed in **Table 4.1**. BE values of Co2p<sub>3/2</sub> from the heterogenized multilayers and clusters of CoTPP on silicon wafer (Entry 2, 781.5 eV) were higher than for monolayer attached CoTPP on the gold surfaces (Entry 1, 780.0 eV) in the magnitude of +1.5 eV. This difference decreases to +0.8 eV when the material has been used in the HQ oxidation reaction (Entry 3, 780.8 eV). Since the clusters and multilayers of CoTPP were observed with the AFM to decrease upon utilization in the HQ oxidation reaction together with the decrease in BE difference towards Co on gold we assumed a correlation between high Co2p<sub>3/2</sub> BE values to clusters and multilayers of CoTPP. Since the BE values of Co2p<sub>3/2</sub> on silica particles (Entry 4, 779.5 eV) were lower than on both gold and silicon wafer we proposed that the heterogenized CoTPPs were chemisorbed more as a monolayer than cluster and multilayer. Such conclusions based on binding energies from different kinds of substrates are not straightforward, but the proposition is more supported later on.

**Table 4.1** Observed Co2p<sub>3/2</sub> binding energy values obtained from XPS measurements on CoTPP immobilized on gold, silicon wafer and silica particles together with the catalyst organization.

Entry	Sample	Co2p <sub>3/2</sub> (eV)	ΔE@ Au (eV)	Catalyst Organization
1	CoTPP/Au	780.0 <sup>[a]</sup>	±0	monolayer
2	CoTPP/Si wafer	781.5	+1.5	multilayer/cluster
3	CoTPP/Si wafer <sup>[b]</sup>	780.8	+0.8	multilayer/cluster <sup>[d]</sup>
4	CoTPP/Si particle <sup>[c]</sup>	779.5	-0.5	monoattached <sup>[e]</sup>

<sup>[a]</sup> Data from reference 41. <sup>[b]</sup> After utilization in the reoxidation reaction of BQ.

<sup>[c]</sup> Silica particles were dried onto a piece of conductive glass prior to XPS measurements. <sup>[d]</sup> Observed cluster/multilayer decrease with AFM. <sup>[e]</sup> Predicted by comparing the Co2p<sub>3/2</sub> binding energies.

#### 4.2.3 Catalyst Activity - Oxidation of Hydroquinone

The activity of the heterogenized CoTPPs was evaluated by following the oxidation reaction of hydroquinone (HQ) to *p*-benzoquinone (BQ) by CoTPP with molecular oxygen as terminal oxidant, see **Figure 4.1**. Catalyst activity was measured by UV/vis quantification of BQ in the reaction solution. The final selectivities of the oxidation reactions were

determined by NMR analysis to be 99% as no other products were detected.

#### 4.2.3.1 Turnover Numbers ( $n_{BQ}/n_{CoTPP}$ )

In **Figure 4.4** the CoTPP performance is presented as the turnover number (TON,  $n_{BQ}/n_{CoTPP}$ ) for the homogeneous- (data from reference 41) and heterogeneous catalyst immobilized on gold (data from reference 41), silicon wafer, silica particles and magnetic silica particles. TONs for the heterogeneous conditions have been corrected for the background auto-oxidation reactions. For the CoTPPs heterogenized on the silicon wafers it was found that the TONs were about 10-fold higher than for the homogeneous mononuclear CoTPPs and the life time was maintained for 18 days or over 400 hours whereas the homogeneous congener was deactivated already after 24 hours. However, the activity of the silicon wafer immobilized CoTPPs was around 10 times lower than that for the same catalyst immobilized on the gold surface. One plausible explanation for the lower activity on the silicon wafer is the observed clusters and multilayers of surface confined catalysts as it is generally only the catalyst molecules present in the upper most layer e.g. the surface catalyst molecules that participate in the oxidation reaction. The bulk catalyst molecules are assumed to be almost completely inactive. An overestimation in quantity of the active molecules and subsequently also an underestimation of the actual activity of the active molecules is thus made.

The activity of the heterogenized CoTPPs on both silica particles and magnetic silica particles were found to be almost the same as on gold and consequently 10 times higher than that on silicon wafers as it was increased 100-fold compared to the homogeneous CoTPPs. The CoTPPs immobilized on silica particles showed also the long term stability as heterogenized on the other support surfaces. As we were able to achieve the same catalytic activity for the heterogenized CoTPP on the silica particles as for the monolayer of catalysts organized on gold the possibility of a synergistic effect between CoTPP and gold could be excluded. Our proposal that the catalyst attached to silica particles was arranged as single active units was further promoted than just comparing the  $Co2p_{3/2}$  binding energies obtained on the different supports. A high background hydroquinone oxidation for the magnetic silica particles was observed, which was found to be negligible for the silica particles.

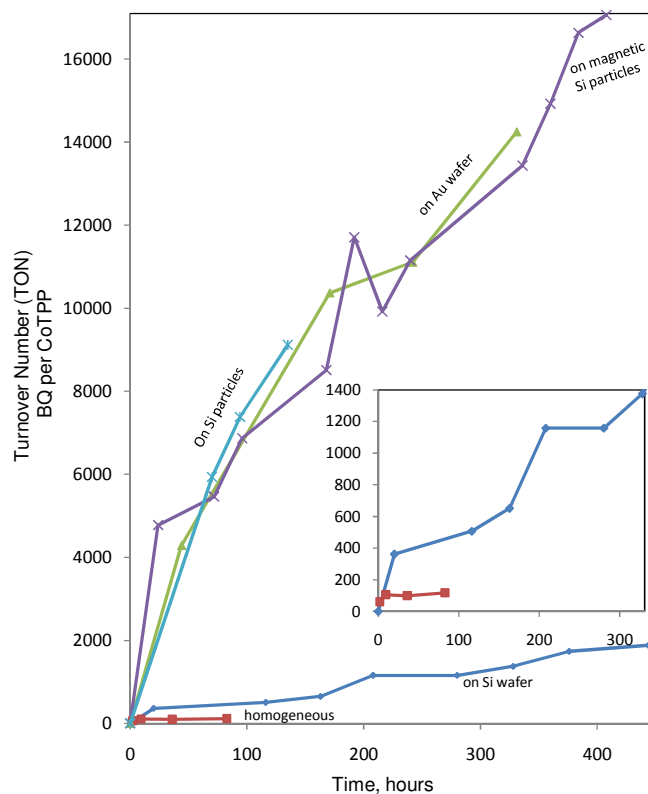


**Figure 4.4** Turnover numbers (TONs) for CoTPP under homogeneous- and heterogeneous conditions immobilized to gold, silicon wafer, silica- and magnetic silica particles in BQ reoxidation reaction. TONs for homogeneous conditions and heterogeneous conditions on gold data from reference 41. The inset is an enlargement of the lower part of the graph where TON values are plotted after homogeneous CoTPP catalysis (the lower curve) and heterogeneous CoTPP catalysis (the upper curve) immobilized on silicon wafers. TONs for the heterogeneous conditions have been corrected for the background auto-oxidation reactions.

#### 4.2.3.2 Initial-, Stabilized Turnover Frequencies and Catalyst Reusability

The initial turnover frequencies (TOFs,  $n_{BQ}/n_{CoTPP} \cdot h^{-1}$ ) e.g.  $TON \cdot h^{-1}$ , for the different heterogenized catalysts are summarized in **Table 4.2** and compared with reported TOFs for other metal macrocycles used in hydroquinone oxidations such as cobalt salophen (Co salophen) and iron phthalocyanine (FePc). As seen in the table, TOFs obtained for the

heterogenized CoTPP on gold, silica- and magnetic silica particles are among the highest reported for metal macrocycles in HQ oxidation with molecular oxygen. Heterogenization of homogeneous CoTPP seems to boost its oxidative activity significantly which similarly have been reported for heterogenized FePc encapsulated in zeolites (FePc/ZeY)<sup>32</sup>. Since the heterogenized CoTPPs have been utilized in long term reactions e.g. up to 400 hours it would be desirable not only to evaluate the initial oxidation rates whereas stabilized TOFs are also displayed in table 4.2. The TOFs measured when the oxidation rates are constant after an oxidation time of 100-180 hours for CoTPP heterogenized on gold, silica- and magnetic silica particles are comparable with the initial TOFs for homogeneous CoTPPs and Co salophens. The latter catalysts are deactivated after a few hours.

**Table 4.2** Initial TOFs and stabilized TOFs obtained for various metal macrocycles at homogeneous and heterogeneous conditions in BQ reoxidation with molecular oxygen.

Entry	Heterogeneous	Reference	TOF <sub>initial</sub>	TOF <sub>stabilized</sub>
1	CoTPP/Au	ref. [41]	97	24 <sup>[a]</sup>
2	CoTPP/Si wafer	this work	18	4
3	CoTPP/Si particle	this work	85	18
4	CoTPP/SiFe <sub>2</sub> O <sub>3</sub> particle <sup>[b]</sup>	this work	76	18
5	FePc/ZeY	ref. [32]	24	N.A. <sup>[c]</sup>
Entry	Homogeneous	Reference	TOF <sub>initial</sub>	TOF <sub>stabilized</sub>
6	CoTPP	ref. [41]	29	0.4
7	Co(salophen)	ref. [15]	28	N.A. <sup>[c]</sup>
8	FePc	ref. [32]	10	N.A. <sup>[c]</sup>

<sup>[a]</sup> Calculated from reference 41. Average TOF between 170-330h. <sup>[b]</sup> Fe<sub>2</sub>O<sub>3</sub> = magnetite; magnetic particle. <sup>[c]</sup> Data not available.

The reusability or the recyclability was evaluated for the CoTPP/silica particle catalyst after an initial oxidation time of 135 h, whereas the initial TOF was decreased from 85 turnover numbers per hour to 46 turnover numbers per hour. However the TOF after long use (100-180 h) for the reused CoTPP/silica particle catalyst was around the same as for the CoTPP/magnetic silica particle catalyst indicating that long term turnover frequencies are maintained upon reuse, see **Figure 4.5**.

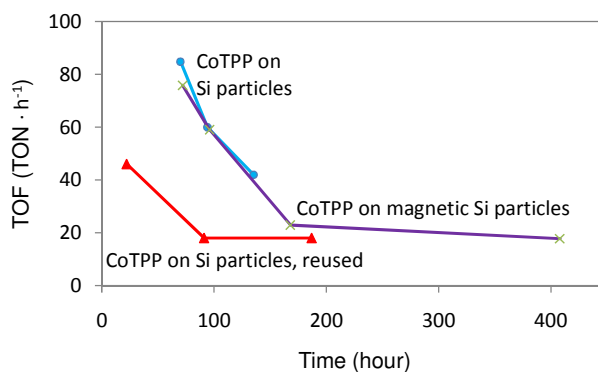


**Figure 4.5** Turnover frequencies for CoTPP immobilized on magnetic silica particles for the first use and for CoTPP immobilized on silica particles for the first and second use showing the reusability.

### 4.3 Conclusions and Further Perspectives

Heterogenization of the homogeneous oxidation catalyst CoTPP was found to circumvent the problem with catalyst deactivation in solution as the activity and life time were dramatically boosted upon the immobilization. The organization and orientation of the surface-confined catalyst molecules were found to be important for the oxidation activity as the catalysts organized as monolayer or mono-units displayed higher activity than the aggregates and multilayer organizations. Extending the system from flat solid surfaces as supports to solid spherical particles increases the active surface area at the same time as the volume can be reduced, which removes the limitations for scale-up. The high catalyst activity previously reported on gold surfaces could be obtained also on silica particles. CoTPP heterogenized on gold or on silica particles displayed significant hydroquinone oxidation rates during 400 hours, which could be maintained upon reuse compared to homogeneous CoTPP and Co salophens. The initial rates of the latter were lower and tended to decline already after a few hours. On the silica particles, we were only able to achieve loadings of CoTPP of 98 ppm (weight/weight) as a maximum, probably due to a base promoted disulfide formation resulting in a polymerization of the CoTPP molecules in solution. For scale-up purposes it is desirable to increase these catalyst loadings significantly.

## 5. Manufacturing of Anisotropic Particles by Site Specific Oxidation of Thiols (Paper III)

### 5.1 Introduction

Previously our group were able to introduce surface anisotropy on flat silicon surfaces functionalized with thiols by site specific electrochemical oxidation of the surface-confined thiols to more reactive thiolsulfonates which subsequently were conjugated with thiol-molecules<sup>103</sup>, see section 2.2.2 on electrochemical oxidation of surface confined thiols. In this manner, they were able to manufacture patterns of surface-confined molecules and particles with micrometer<sup>104</sup>- and nanometer<sup>105</sup> resolution. In these studies, the surfaces of interest e.g. the thiol-functionalized silicon surfaces were used as working electrodes and the patterns were made by positioning a combined reference/auxiliary electrode in the vicinity of the surfaces during the application of a suitable potential.

Supported by this technique based on the surface-confined electrochemistry we wanted to extend the studies involving also particles in order to produce so called anisotropic particles. Since the oxidation of thiols present on particles is not as straightforward as for thiols immobilized on a flat surface, the possibilities of oxidizing nonconductive particles, present in a solution, at the electrolyte-working electrode interface had to be explored. While this can lead to the formation of anisotropic particles, homogeneous thiol oxidation is clearly expected for conductive particles. To attract the particles to the working electrode we employed nonconductive paramagnetic polymeric particles and external magnets.

Anisotropic particles exhibit some interesting properties as they are multifunctional surfaces whereas bimetallic particles with particles-on-particle morphologies can be considered as anisotropic particles which recently have shown to reveal very exciting qualities as heterogeneous catalysts<sup>1,2,76</sup>.

## 5.2 Results and Discussion

### 5.2.1 Preparation of the Anisotropic Particles

Initially the particle surfaces needed to be modified with thiols. Amino-functionalized magnetic polymeric beads were reacted with SPDP and DTT as described in section 2.1.2 for introduction of thiols on amino-functionalized surfaces. The extent of the thiol modification was evaluated according to 2,2'-dipyridyl-disulphide (2PDS) coupling, see section 2.1.3 on determination of the thiol concentration, to correspond to  $10^8$  thiols per particle.

The particles were then employed in a three-electrode setup comprising a glassy carbon- or a gold surface as the working electrode, Pt reference electrode and a gold wire as the auxiliary electrode. A cylindrical reaction cell was mounted on the working electrode in which the electrolyte together with the particles as well as the reference- and auxiliary electrodes were placed. Attraction of the particles to the working electrode was obtained by placing an external magnet under the working electrode, see **Figure 5.1a**. When applying a sufficiently positive potential to the working electrode with respect to the reference electrode an oxidation at the working electrode/solution interface will take place. This results in an oxidation of the thiols yielding thiolsulfonates or thiolsulfinates. As the particles are spherical only the thiols closest to the working electrode will be oxidized leaving the other surface thiols unoxidized generating a surface-confined patch containing reactive structures, see **Figure 5.1b**. By subsequently attracting, oxidizing and releasing the particles repeated times the possibilities to produce several patches on the particles were also explored.

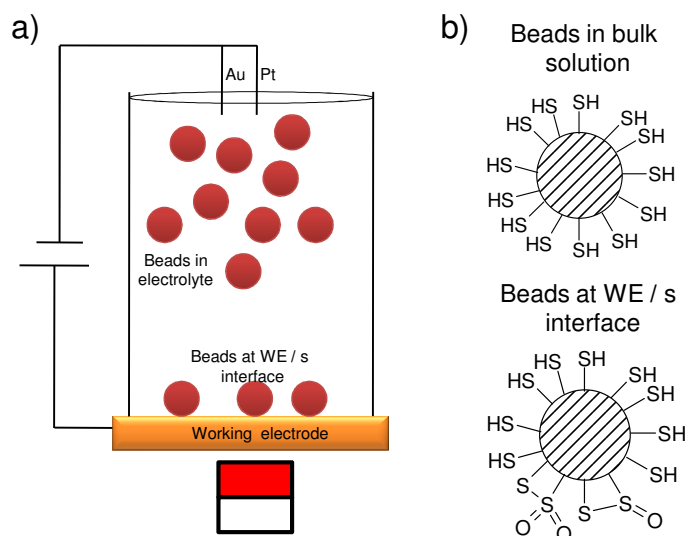


**Figure 5.1** Schematic figures of the electrochemical approach employed to generate anisotropy on particle surfaces. **(a)** Nonconductive magnetic polymeric particles modified with thiols are attracted from the bulk electrolyte to the surface of the working electrode by magnetic forces. **(b)** Only thiols in contact with the working electrode are oxidized to thiosulfonates or thiosulfonates generating reactive patches on the particles. The particles present in the bulk electrolyte are not oxidized.

### 5.2.2 Characterization of the Anisotropic Particles

The prospect of oxidizing thiols to thiosulfinates or thiosulfonates immobilized on a separate surface by enclosing the surface on-top of the working electrode, rather than comprising them immobilized on the working electrode as previously described, was evaluated with XPS analysis. Since it can be hard to analyze isolated patches of thiosulfonates and thiosulfinates on particle surfaces with XPS, a flat thiolated nonconductive silicon surface was instead investigated after oxidizing it employing the same approach as for the particles, i.e. by placing the thiol-surface on a glassy carbon working electrode.

### 5.2.2.1 X-ray Photoelectron Spectroscopy Study

In **Figure 5.2** XP sulfur 2s (S2s) spectra acquired on the flat thiolated silicon surfaces before (a) and after (b) the electrochemical oxidation are displayed. The peak at a binding energy (BE) of approximately 228 eV is typical for surface thiols whereas the broader peak at a BE of about 232.5 eV is seen for oxidized thiols such as thiolsulfinates and thiolsulfonates, for which the BEs are around 231 eV and 233 eV, respectively<sup>104</sup>. Based on this it was concluded that surface thiols present in contact with the glassy carbon working electrode were oxidized mainly to thiolsulfonates when a potential of +2.31 V vs. Ag/AgCl was applied during 60 s.

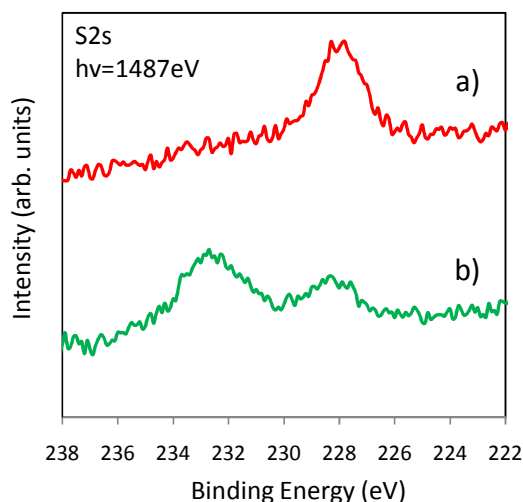


**Figure 5.2** The sulfur 2s XP spectrum acquired for a nonconductive thiolated silicon surface prior (a) and after (b) electrochemical oxidation on the surface of a glassy carbon working electrode at a potential of +2.31 V vs. Ag/AgCl during 60s.

### 5.2.2.2 Fluorescence Microscopy Study

The reactive patches of thiolsulfonates and thiolsulfinates on the particle surfaces were visualized by coupling with fluorescent labeled thiol-proteins and using subsequent investigations in a fluorescence microscope where the patches appear as fluorescent spots on the particles. **Figure 5.3a** depicts fluorescence microscopy images of particles

comprising one fluorescent spot, which were obtained by oxidation at +1.61 V vs. Ag/AgCl using a glassy carbon working electrode. At higher potentials the fluorescent spots were absent, probably due to an overoxidation of the surface thiols.

Further, particles were also subsequently attracted, oxidized and released repeated times in order to explore the possibilities of obtaining several patches on each particle. The results are depicted in **Figure 5.3b**. We found particles with zero to four patches when this attract-release-oxidize approach was repeated up to four times using a gold working electrode. This clearly shows that multifunctional particles can be obtained with the present approach. It was also found that a homogeneous oxidation of the entire particle surface could be obtained when the particles were oxidized on the gold working electrode depending on the composition of the electrolyte used. The homogeneous oxidation could be explained by a release of oxidizing  $\text{Au}^{\text{III}}$  species from the metallic gold surface in agreement with previous reports<sup>107,108</sup>. This phenomenon is more explored, discussed and even used in different applications later on in this thesis e.g. see Paper **IV** and **V**. Using an image processing and analyzing program, the areas of the electrochemical generated particle surface confined patches were evaluated to be  $0.47 \pm 0.05 \mu\text{m}^2$  employing the glassy carbon electrode and  $2.03 \pm 1.01 \mu\text{m}^2$  utilizing the gold electrode. These values correspond to approximately 2 and 10 %, respectively, of the particles surface as the particles had a diameter of 5  $\mu\text{m}$ .

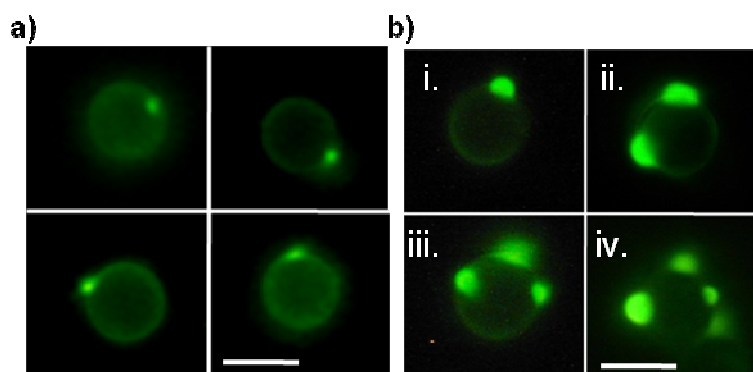


**Figure 5.3** Fluorescence microscopy images of nonconductive magnetic polymeric particles containing surface confined thiols which were electrochemical oxidized on (a) a glassy carbon electrode at +1.61 V vs. Ag/AgCl for 60s and (b) a gold working electrode at +1.0 V vs. Ag/AgCl for 0.1 s followed by conjugation with fluorescent labeled thiol-proteins yielding anisotropic particles. The glassy carbon oxidation was carried out using a single potential pulse yielding one patch whereas the gold electrode experiments involved up to four potential pulses yielding i. one ii. two iii. three iv. four visible patches. The lengths of the scale bars correspond to 5  $\mu$ m.

### 5.2.3 The Conversion Dilemma

A dilemma with this electrochemical approach for site specific oxidation of magnetic particle-surface-confined thiols is that the number of particles exhibiting patches was rather low after the oxidation step, corresponding to around 3-5% of the total number of particles. Intense work was hence carried out to find the most significant reasons for these low conversion degrees. One possible reason is the choice of chemistry since the generated thiolsulfonates and thiolsulfinates are reactive towards any kind of thiols, not only thiol-proteins. There is hence a possibility that the modified particles react with one another to generate clusters. To circumvent this generation of clusters, the oxidized particles should be separated from each other in the reaction solution. Surface migration of the particles can, however, not be excluded and the particles can also interact with one another during the surface release or desorption step.

Another plausible explanation for the low yield could be that only a low percentage of the particles are in contact with the working electrode

during the applied potentials. In the presence of the permanent magnet the paramagnetic particles was observed in an optical microscope to form chains containing 5-10 particles, which were pointing vertical away from the working electrode surface.

### *5.3 Conclusions and Further Perspectives*

Surface-confined thiols immobilized on nonconductive magnetic particles present at the surface of a working electrode can be oxidized to thiolsulfonates and thiolsulfonates thus generating reactive patches on the particle surfaces yielding anisotropic particles. This is the first report on the use of electrochemistry for the preparation of such anisotropic particles. The method is inexpensive, straightforward and allows for large-scale manufacturing as around  $10^6$  particles can be modified in parallel. By employing electrochemistry it is possible to control the size of the particle-surface-confined patches by varying the magnitude and time of the potential pulses.

The particle-surface-confined patches of thiolsulfonates and thiolsulfonates can be further functionalized to provide interesting properties of the particles useful in different kinds of applications. In our work we have functionalized the particles with thiol-proteins labeled with fluorescein isothiocyanate (FITC) for visualization in a fluorescence microscope, but it would also be possible to functionalize the particles with almost any kind of thiols or to produce the surface-confined patches on almost any kind of a thiolated particle. The approach with several patches on each particle and additional immobilization with thiol-functionalized antigens open up the possibility for using the anisotropic particles as barcodes in multiplex diagnostics, whereas functionalization with thiol-enzymes could introduce multi-catalytic capacity. Heterogenization on an anisotropic metal oxide particle with thiol-nanoparticles could generate bimetallic catalysts with particles-on-particle morphology exhibiting attractive metal-oxide interfaces as well as particles serving as bi-functional catalysts. The possibilities are numerous and the anisotropic particles should hence be considered as very promising functional materials for future inventions.

## 6. Electrochemical Synthesis of Gold and Protein Gradients on Particle Surfaces and of Dispersed Gold Nanoparticles Supported in the Pores of Siliceous Mesocellular Foam: An Efficient Catalyst for Cycloisomerization of 4-Pentynoic Acids to Lactones (Paper IV and V)

### 6.1 Introduction

In the previous work, paper III, we were able to perform site specific electrochemical oxidation of particle-surface-confined thiols on the surfaces of glassy carbon or gold working electrodes subsequently resulting in patchy-like anisotropic particles. The particle-surface-confined patches of thiolsulfonates and thiolsulfonates were further conjugated with thiol-proteins to yield functional anisotropic particles. The functionalization is, however, not only restricted to proteins as almost any kind of thiol-ligands could be conjugated to the thiolsulfinate- and thiolsulfonate patches. When the gold working electrode was used we found homogeneous oxidation of the particle surface thiols when chloride ions was present in the electrolyte due to the formation of oxidizing  $\text{Au}^{\text{III}}$  chloride species<sup>107,108</sup>.

In this work, we explored the surfaces of homogeneous oxidized magnetic particles with XPS and detected the presence of surface confined  $\text{Au}^{\text{I}}$  species. The latter result from a redox reaction between the dissolved  $\text{Au}^{\text{III}}$  species and the surface confined thiols present on the particles yielding thiol supported  $\text{Au}^{\text{I}}$ . For relative short potential pulses, surface-confined gradients of  $\text{Au}^{\text{I}}$  could be obtained, i.e. intra particle gradients, whereas the entire particle surfaces could be modified with  $\text{Au}^{\text{I}}$  for longer oxidation steps. Since the extent of modification depends on the distance between the particles and the gold electrode, the latter

approach can be used to generate particles with different gold coverages, i.e. inter particle gradients. Visualization of the gradients was made by functionalizing the particles with fluorescent proteins, consequently generating gradients of proteins on the particle surfaces, followed by investigations using fluorescence microscopy. Further, the formation of surface confined Au<sup>I</sup> gradients was also studied using flat silicon surfaces which then were characterized by means of XPS.

Surface-confined thiol-supported Au<sup>I</sup> species were also produced on siliceous mesocellular foam (MCF) and chemically reduced to obtain well dispersed thiol-stabilized gold nanoparticles of 1-8 nm size. It was found that these gold nanoparticles could be used as efficient catalysts for the cycloisomerizations of 4-pentynoic acids to lactones.

## *6.2 Results and Discussion*

### *6.2.1 Particle-Surface-Confined Au<sup>I</sup> Gradients*

#### *6.2.1.1 Preparation of Au<sup>I</sup> and Protein Gradients on Particles*

The amino terminated magnetic polymeric particles were modified with thiols as previously described, involving SPDP conjugation followed by DTT reduction. The amount of thiols on the particles was determined to be approximately 10<sup>8</sup> thiols per particle by the use of 2PDS. Thiolated magnetic polymeric particles were then employed in the same electrochemical set-up as described in paper III comprising a gold working electrode with a phosphate buffered saline solution (PBS, 10 mM, pH 7.2) containing 0.15 M sodium chloride (NaCl) serving as the electrolyte. The thiolated magnetic particles were attracted to the gold working electrode surface by magnetic forces. Applying a potential of +0.9 V vs. Pt reference electrode generated a release of oxidizing Au<sup>III</sup> species in the form of gold(III)chloride in the vicinity of the gold working electrode. These gold(III)chloride species diffused into the electrolyte and reacted with the thiols to generate disulfides and thiol-supported Au<sup>I</sup> (S<sup>-I</sup>-Au<sup>I</sup>) on the surface of the particles. Formation of gold(I)thiolates by reaction of gold(III)chloride with thiols is frequently used for the production of thiol-stabilized gold nanoparticles<sup>100</sup>. The gradients of particle-surface-confined Au<sup>I</sup> resulted from the particles spherical shape which caused the surface-bound thiols to be located at different positions

in the  $\text{Au}^{\text{III}}$  chloride diffusion layer. Particle surface thiols close to the metallic gold working electrode were hence exposed to a higher  $\text{Au}^{\text{III}}$  concentration (i.e. a higher redox potential) than surface thiols located on top of the particles thus generating a gradient. The particle-surface-confined  $\text{Au}^{\text{I}}$  gradients were further used to obtain protein-thiols via the interaction between  $\text{Au}^{\text{I}}$  and thiol yielding protein gradients on the particle surfaces. A schematic figure of the electrochemical process involving the generation of the  $\text{Au}^{\text{I}}$  and protein gradients on the particle surface are displayed in **Figure 6.1**.

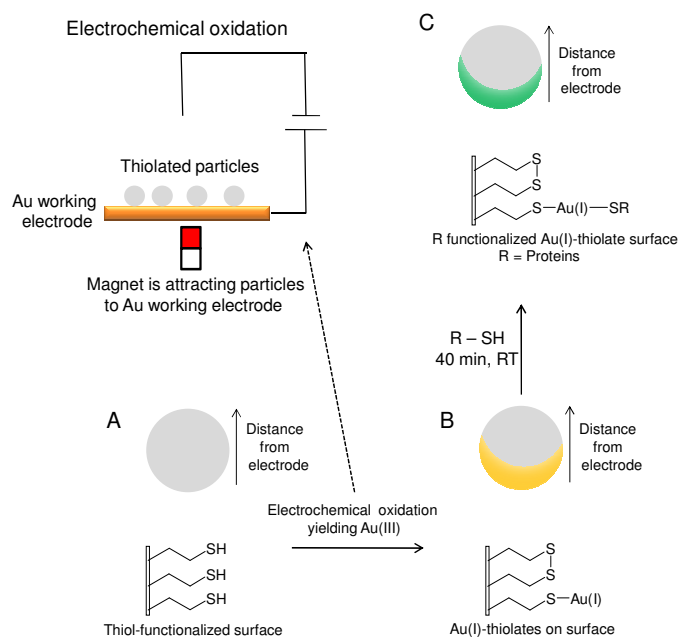


**Figure 6.1** Preparation of surface-confined protein gradients on magnetic polymer particles. (A) Thiol-functionalized magnetic particles are oxidized by released  $\text{Au}(\text{III})$  chloride complexes to yield (B) a particle-surface-confined gradient of  $\text{Au}^{\text{I}}$ . (C) Thiol-proteins are conjugated to the gold(I)thiolates to generate a surface density protein gradient.

#### 6.2.1.2 Electrochemical Study - Oxidation of $\text{Au}^0$ to Soluble $\text{Au}^{\text{III}}$ Species

The release of oxidizing  $\text{Au}^{\text{III}}$  species from the surface of the gold working electrode can be seen in the cyclic voltammogram recorded with the three-electrode set-up comprising a gold working electrode, Pt quasi-

reference electrode and a gold auxiliary electrode with a chloride-containing PBS electrolyte (10 mM, pH 7.2, 0.15 M NaCl) employing a scan-rate of 50 mV/s, see **Figure 6.2**. As the oxidation current of gold ( $\text{Au}^0 \rightarrow \text{Au}^{\text{III}} + 3\text{e}^-$ ) initiated at around +0.7 V is significantly larger than the reduction current ( $\text{Au}^{\text{III}} + 3\text{e}^- \rightarrow \text{Au}^0$ ) commenced at around +0.3 V, generation of soluble  $\text{Au}^{\text{III}}$  species is to be expected. The release of  $\text{Au}^{\text{III}}$  from gold electrodes in the presence of complexing agent such as chloride is well-documented in previous reports<sup>107,108</sup>. The generation of soluble  $\text{Au}^{\text{III}}$  species was quantified with inductively coupled plasma - mass spectrometry (ICP-MS) by detection of gold in the electrolyte. It was found that approximately 80  $\mu\text{g}$  of Au was released from the working electrode when a potential of +0.9 V vs. Pt was applied during 60 seconds. Further, no gold was detected in the electrolyte with ICP-MS once chloride was excluded from the PBS solution.

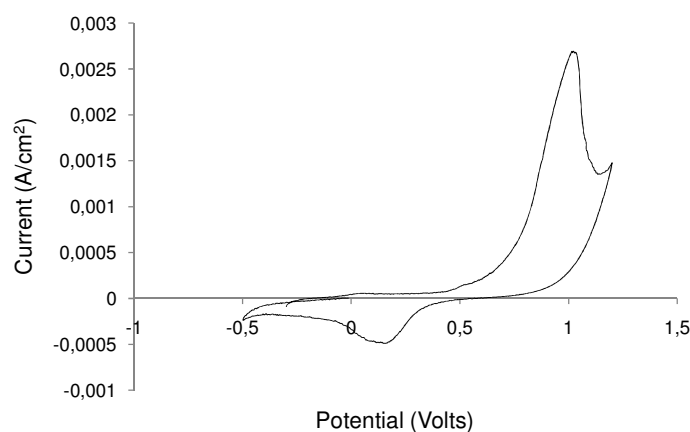


**Figure 6.2** Cyclic voltammogram acquired for a gold electrode in a PBS buffer containing 0.15 M NaCl employing a scan-rate of 50 mV/s. The gold oxidation current is larger than the gold oxide reduction current indicating a generation of soluble gold(III) chloride species.

#### 6.2.1.3 X-ray Photoelectron Spectroscopy Study - Detection of Surface-Confin ed $\text{Au}^{\text{I}}$

The surfaces of thiolated magnetic particles employed in the electrochemical oxidation of the metallic gold working electrode were explored with XPS. Prior analysis the particles were dried onto a piece of conductive glass. X-ray photoelectron spectra of the  $\text{Au}4\text{f}_{7/2}$  and  $\text{Au}4\text{f}_{5/2}$

doublets acquired on the gold-oxidized particles and on a metallic gold surface ( $\text{Au}^0$ ) are seen in **Figure 6.3**. The binding energy for  $\text{Au}4f_{7/2}$  at 85.5 eV obtained for the electrochemically gold-oxidized particles are typical values for gold(I)-thiolates<sup>109</sup> indicating the presence of surface confined  $\text{Au}^{\text{I}}$ , see **Figure 6.3b**. XPS investigation of thiolated magnetic particles resulted in no  $\text{Au}4f$  signal indicating the absent of surface confined  $\text{Au}^{\text{I}}$ .

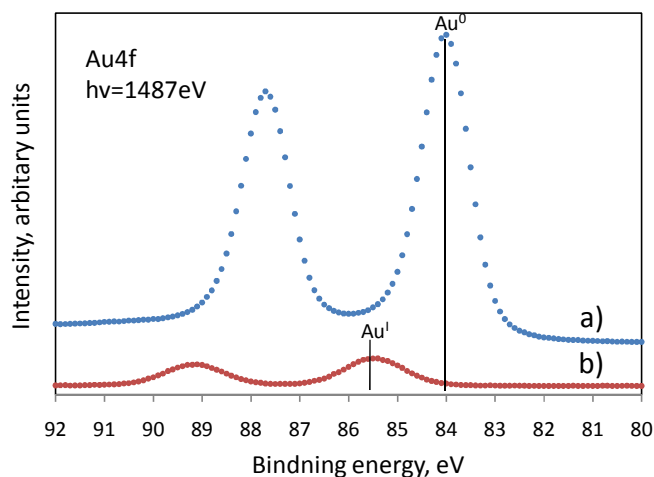


**Figure 6.3** X-ray photoelectron spectra depicting the  $\text{Au}4f_{7/2}$  and  $\text{Au}4f_{5/2}$  doublet acquired on (a) a metallic gold surface e.g.  $\text{Au}^0$  and (b) on the electrochemically gold-oxidized magnetic particles. The  $\text{Au}4f_{7/2}$  binding energy at around 85.5 eV is typical for gold(I)-thiolates indicating the presence of surface confined  $\text{Au}^{\text{I}}$  species on the particles.

#### 6.2.1.4 Fluorescence Microscopy Study - Characterization of Particle-Surface-Confined Gradients and Comparison with the Diffusion Layer Thickness

The surface-confined  $\text{Au}^{\text{I}}$  on the particle were further functionalized with fluorescent thiol-proteins for visualization in a fluorescence microscope consequently generating protein gradients on the particles. Fluorescence microscopy images of such particles electrochemically gold-oxidized at +0.9 V during 0.1, 1 and 10 seconds, respectively, are displayed in **Figure 6.4**. For sufficiently short oxidation times e.g. 0.1s, see figure 6.4a and b, gradients in fluorescence were obtained indicating the

presence of gradients of surface-confined Au<sup>I</sup> on the particles, i.e. intra-particle gradients. For longer oxidation times, e.g. 1 and 10 s, see figure 6.4c and d respectively, the entire particle surfaces were instead fluorescent with a higher intensity being seen for the longer oxidation time. The latter indicates a higher degree of protein functionalization which consequently also indicates a higher gold coverage on the particles. This demonstrates the possibility of generating particles with different surface concentrations of gold and proteins, i.e. inter-particle gradients.

The diffusion layer thickness for the generated oxidizing Au<sup>III</sup> species, i.e. how far the Au<sup>III</sup> species have diffused from the electrode surface in a certain time, can be estimated with the following equation:

$$\Delta = (2 \cdot D \cdot t)^{1/2}$$

wherein  $\Delta$ ,  $D$  and  $t$  represents the distance, the diffusion coefficient and time, respectively<sup>110</sup>. When assuming a diffusion coefficient at  $10^{-6} \text{ cm}^2/\text{s}$ , typical for a small species in an aqueous solution, and an oxidation time of 0.1s, the average distance traveled is estimated to be around  $4.5 \mu\text{m}$ . Since this should be compared with the diameter of the particles of  $4.9 \mu\text{m}$ , it is clear that a gradient of surface confined Au<sup>I</sup> may be expected. For the longer oxidation times of 1 s and 10 s the corresponding distances are estimated to be approximately  $14 \mu\text{m}$  and  $45 \mu\text{m}$ , respectively, indicating that the entire particle should be oxidized. These straightforward calculations are hence in good agreement with our fluorescence microscopy findings.

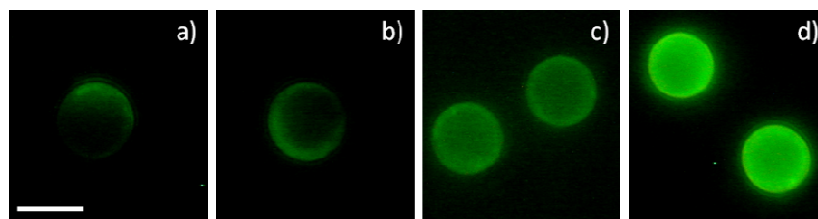


**Figure 6.4** Fluorescence microscopy images of protein- and gold gradients on particles electrochemically gold-oxidized at +0.9 V during 0.1s (**a**) and (**b**), 1s (**c**) and 10s (**d**), respectively. Gradients on the particle in (**a**) and (**b**) whereas the stronger fluorescence in (**d**) compare to **c**) indicates a higher degree of functionalization. The length of the scale bar corresponds to  $5 \mu\text{m}$ .

### 6.2.2 Surface Confined Au<sup>I</sup> Gradients Modeled on Flat Surfaces

In order to mimic the surface-confined gradients on the particle surfaces and to estimate how the concentration of the Au<sup>I</sup> species varies depending on the position in the diffusion layer, gradients were also produced on flat silicon surfaces. These silicon surfaces were first thiolated with mercaptosilane as described in section 2.1.1 on introduction of thiols on silicon surfaces. To achieve surface thiols positioned at different locations in the oxidative Au<sup>III</sup> diffusion layer the silicon surface was tilted against the gold working electrode and the inner wall of the Teflon beaker at an angle of approximately 26°. This preparation was then employed in the previously described three-electrode set-up with an applied potential of +0.9 V vs. Pt during 60 seconds.

#### 6.2.2.1 X-ray Photoelectron Spectroscopy Study - Estimation of the Gold Density Profile

XPS analysis was used to probe the local density of adsorbed Au<sup>I</sup> species along the silicon surface by measuring the Au 4f signals at four different positions, i.e. 0.5, 2.5, 4.0 and 4.5 mm from the gold working electrode surface. The photoelectron spectra for the Au 4f<sub>7/2</sub> and Au 4f<sub>5/2</sub> doublet are displayed in **Figure 6.5a** showing a decrease in the signal intensity as the distance from the gold electrode is increased, the BE of 85.5 eV for Au 4f<sub>7/2</sub> is in good agreement with the values obtained previously for the particle confined gold(I) thiolates. The Au 4f<sub>7/2</sub> and Au 4f<sub>5/2</sub> doublets were integrated to study the dependence of the peak area on the distance from the gold electrode, see **Figure 6.5b**. As the peak areas are proportional to the surface density, the results indicate the presence of a well-defined linear gold gradient according to  $y = 9.6 - 0.63x$  wherein y and x denote the integrated peak area and distance (in mm), respectively.

These observations clearly indicate that the present straightforward electrochemical approach can be used to produce linear gold gradients which in turn can be further functionalized with thiol containing molecules, such as enzymes, to generate e.g. catalyst gradients. Since the parameters tilt-angle, oxidation time, applied potential and electrolyte composition are easy to vary it is expected that gradients with well-controlled density profiles can be created.

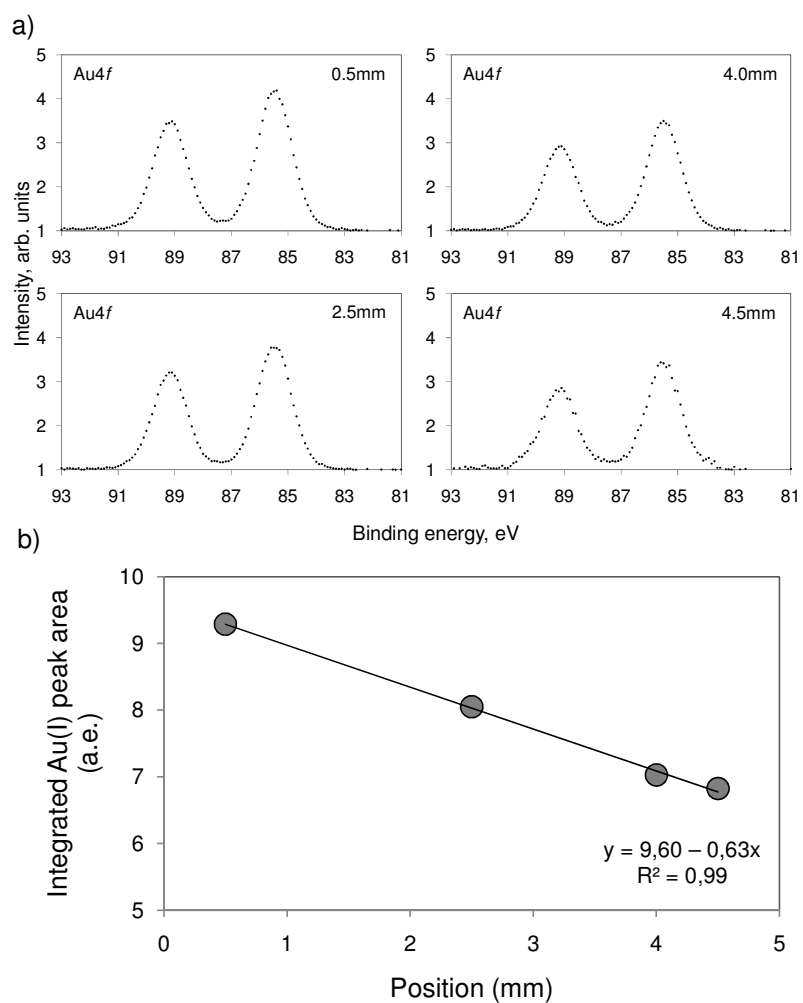


**Figure 6.5 (a)** X-ray photoelectron spectra showing the Au4f<sub>7/2</sub> and Au4f<sub>5/2</sub> doublets acquired for the tilted thiolated silicon surface used in the electrochemical oxidation employing a gold working electrode for four different positions (0.5-4.5mm) from the gold electrode.  $h\nu = 1487$  eV. **(b)** The integrated Au 4f peak area for the four different positions as a function of the distance to the gold electrode. A linear gradient of surface confined gold species is seen to be obtained when the silicon surface is tilted.

### 6.2.3 Preparation of Thiol-Stabilized Gold Nanoparticles Supported on Siliceous Mesocellular Foam

Instead of generating gradients of surface-confined gold species or further functionalizing them with thiol-proteins we also explored the potential of making heterogenized gold metal nanoparticles (AuNPs) by chemical reduction of the thiol-supported  $\text{Au}^{\text{I}}$  to  $\text{Au}^0$  by addition of sodium borohydride ( $\text{NaBH}_4$ ). Surface confined  $\text{Au}^{\text{I}}$  was produced on thiolated siliceous mesocellular foam (MCF) by the above mentioned electrochemical approach at a potential of +0.9 V vs. Pt during 60s with the idea to cover the entire MCF surface with gold species rather than generate gradients. Initially the aminopropyl functionalized MCF were modified with thiols with SPDP coupling followed by DTT reduction as previously described. The thiol functionalization was determined with 2PDS as previously described to be around 2.1 weight%. The reasons of using aminopropyl-MCF for the heterogenization of  $\text{Au}^{\text{I}}$  are the high surface area that mesoporous materials offers as well as it has recently been used as support for the immobilization of well dispersed Pd nanoparticles which further showed to be a reusable catalyst for alcohol oxidations<sup>111</sup>. After the electrochemical oxidation experiment we simply reduced the MCF surface-confined  $\text{Au}^{\text{I}}$  with  $\text{NaBH}_4$  to obtain the thiol-supported AuNPs. Generally AuNPs are produced by chemical<sup>100</sup> or electrochemical<sup>112</sup> reduction of hydrogen tetrachloroaurate ( $\text{HAu}^{\text{III}}\text{Cl}_4$ ) in presence of stabilizers to circumvent particle aggregations. To the best of our knowledge this is the first time AuNPs are produced from reduction of electrochemically generated heterogenized gold ions. Since the correlation of catalytic activity with particle size is well documented with higher activity for small NPs<sup>43,113</sup> one of the main focus of AuNP production has been to synthesize small and stable particles which consequently possess high catalytic activity therefore it's interesting to explore the properties of our electrochemically made AuNPs. An illustration of the overall process employed to generate the MCF heterogenized AuNPs is shown in **Figure 6.6**.

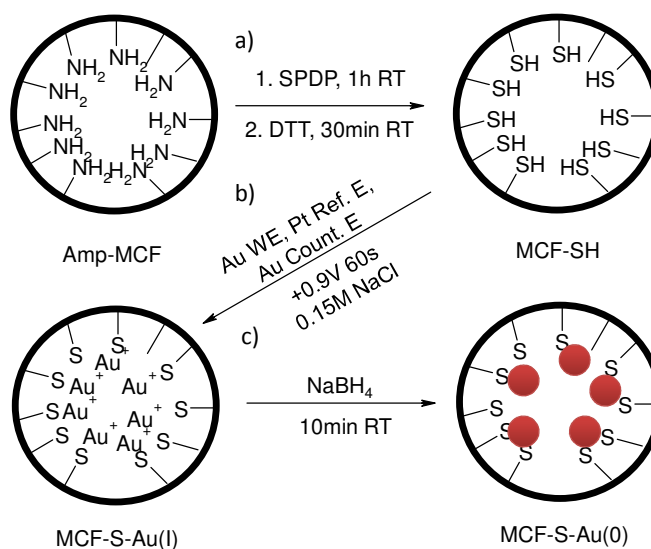


**Figure 6.6** Preparation of thiol-stabilized gold nanoparticles heterogenized on to siliceous mesocellular foam (MCF). **(a)** Amino-MCF is initially modified with thiols by SPDP coupling followed by DTT reduction to obtain MCF-SH. **(b)** Heterogenization of  $\text{Au}^{\text{I}}$  on MCF-SH by the electrochemically based release of oxidative  $\text{Au}^{\text{III}}$  species. **(c)** Reduction with sodium borohydride of  $\text{Au}^{\text{I}}$  to  $\text{Au}^0$  to get the thiol-supported gold nanoparticles immobilized on MCF.

#### 6.2.3.1 Characterization of the Gold Nanoparticles Heterogenized on Siliceous Mesocellular Foam

The heterogenized AuNPs were characterized with Transmission Electron Microscopy (TEM) analysis, see **Figure 6.7**. Based on the TEM images it was found that the AuNPs on MCF varied in sizes from 8 nm down to 1 nm whereas the reference image in **Figure 6.7d** acquired on thiolated MCF indicating no contamination of other metal nanoparticles. The loading of AuNP on MCF was determined with ICP-MS to be approximately 3 weight%.

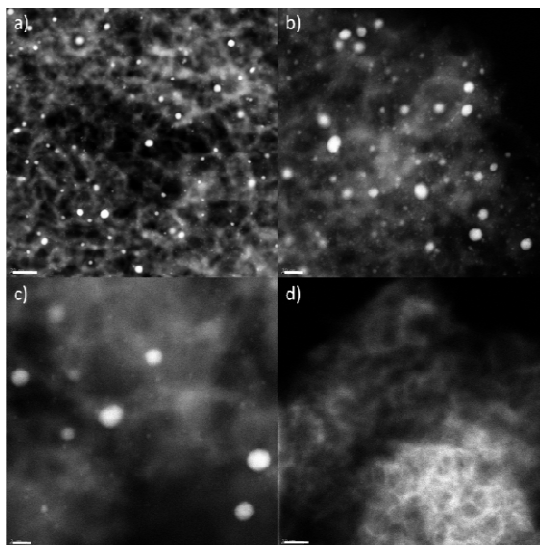


**Figure 6.7** Transmission Electron Microscopy (TEM) images acquired on MCF containing thiol-stabilized AuNPs with the size distribution of 1-8nm in (a), (b) and (c). The MCF immobilized AuNPs were produced by electrochemical oxidation of a metallic gold working electrode surface in presence of the thiolated MCF followed by reduction with sodium borohydride. (d) TEM image on MCF-SH without AuNPs. Scale bars corresponding in a) and d) to 20 nm, in b) to 10 nm and in c) to 5 nm.

#### 6.2.3.2 Cycloisomerization of 4-Pentynoic Acids to Lactones - Heterogeneous Catalysis by Gold Nanoparticles on MCF

The thiol-stabilized AuNPs heterogenized on MCF (Au(0)-MCF) were tested as catalyst in the cycloisomerization reaction of 4-pentyniic acids to the corresponding lactones, see **Table 6.1**. Reactions were run with 0.2 mmol substrate and 0.25 mol% catalyst in 2 ml dichloromethane (DCM) at room temperature (RT) or 40 °C under an atmosphere of air. Conversions were evaluated with  $^1\text{H}$ -NMR spectroscopy.

It was found that the heterogeneous Au catalyst exhibit high activity as substrate **1a** was converted to the corresponding lactone with conversion of 97 % after 1 hour at RT (Table 6.1, entry 1). Adding base ( $\text{NEt}_3$ ) to the reaction did not promote the cycloisomerisation as 90 % conversion was obtained after 1 hour (Table 6.1, entry 1). Addition of a substituent in the  $\alpha$ -position to the carboxylic acid ( $\text{R}^2$ ), substrate **1b**, gave 89 % conversion after 1 hour at RT (Table 6.1, entry 2). Substitution at the alkyne group ( $\text{R}^1$ ) on the other hand significantly affected the intramolecular cyclization as substrate **1c** was cycloisomerized with 89 %

conversion at 40 °C after 14 h (Table 6.1, entry 3). All cyclizations occurred via 5-exo mode with 99 % selectivity as no other products were detected with the NMR.

**Table 6.1** Heterogeneous gold-catalyzed cycloisomerization of 4-pentynoic acids to lactones.<sup>a</sup>

Entry	R <sup>1</sup>	R <sup>2</sup>	substrate	T (°C)	time (h)	conv. <sup>b</sup> (%)	TOF (h <sup>-1</sup> )
1	H	H	<b>1a</b>	RT	1	97, 90 <sup>c</sup>	388, 360 <sup>c</sup>
2	H	Hexyl	<b>1b</b>	RT	1	89, >99 <sup>d</sup>	356
3	<i>p</i> -CF <sub>3</sub> -Ph	H	<b>1c</b>	40	14	89	25
4	<i>p</i> -OMe-Ph	H	<b>1d</b>	40	20	80	16

<sup>a</sup>. Cycloisomerization of 4-pentynoic acids (0.2 mmol) to lactones with 0.25 mol% surface-confined Au catalyst in 2 ml DCM at 1 atmosphere of air. <sup>b</sup>. Conversions determined with <sup>1</sup>H-NMR spectroscopy. <sup>c</sup>. With 0.25 equiv. NEt<sub>3</sub>. <sup>d</sup>. After 3 hours.

Interestingly, substrates **1a** and **1b** were cycloisomerized in the absent of base by the MCF surface-confined Au species in high rates as the TOFs were found to be 388 h<sup>-1</sup> and 356 h<sup>-1</sup>, respectively. Compared to previous reports on the cycloisomerization of  $\alpha$ -substituted 4-pentynoic acids concerning heterogeneous systems for Rh (TOF = 2.2 h<sup>-1</sup>)<sup>114</sup> and Au (TOF = 1.7 h<sup>-1</sup>)<sup>115</sup> which were run at 40 °C and for Pd (TOF = 13 h<sup>-1</sup>)<sup>116</sup> run at RT our results are to the best of our knowledge over 10-times higher than the other transition-metal heterogeneous catalysts. Further, the activity in cycloisomerization of the triple-bond substituted 4-alkynoic acid (substrate **1c**, TOF = 25 h<sup>-1</sup>) is higher than for the  $\alpha$ -substituted 4-pentynoic acids concerning the previous reported heterogeneous systems. Notable, the MCF heterogenized Au catalyst showed even higher activity than homogeneous single-sited Au(I) catalysts as it has been reported that substrate **1a** was cycloisomerized to the corresponding lactone with 96 % yield after 2 hours at room temperature requiring a catalyst concentration of 10 mol% and 0.1 eq. of base<sup>117</sup>.

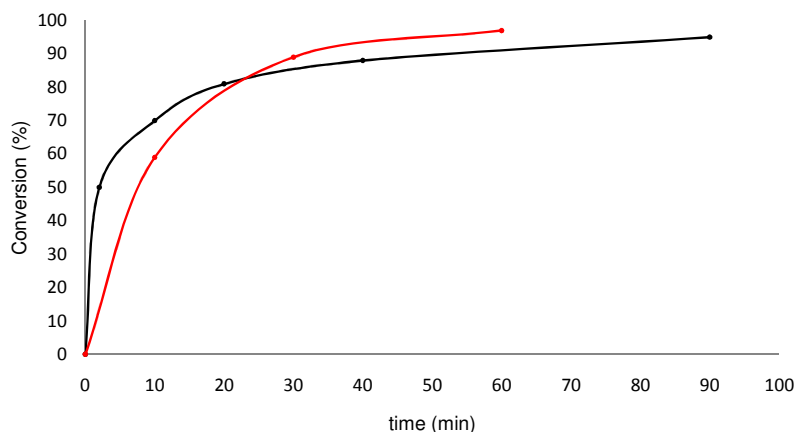


**Figure 6.8** Heterogeneous gold-catalyzed cycloisomerization of 0.2 mmol **1a** with 0.25 mol% surface-confined Au in 2 ml DCM at 1 atmosphere of air in room temperature. (-) with 0.25 eq. NEt<sub>3</sub> and (-) without the base. Conversions determined with <sup>1</sup>H-NMR spectroscopy.

Studying the kinetics for the cyclization of substrate **1a** with the MCF-supported Au catalyst, with and without base, the initial turnover frequencies can be estimated, see **Figure 6.8**. After 10 minutes the initial TOFs are 24 min<sup>-1</sup> and 28 min<sup>-1</sup> for the reactions without and with base, respectively. It appears that the base promotes the reaction at the beginning while it later on seems to inhibit it, compared to the reaction without base. The similar was observed for substrate **1b**, as 50 % conversion were obtained after 3 hours in the presence of NEt<sub>3</sub>. A plausible explanation could be that the nitrogen group coordinates to Au thus causing catalyst inhibition as we recently have observed that primary amines can coordinate to the surface-confined Au<sup>I</sup> species. However, these experimental initial TOFs for the MCF heterogenized Au catalyst are hence remarkable when it comes to cycloisomerizations of 4-pentynoic acids to lactones and further investigations involving other substrates are attending in our laboratory.

Finally, a proposed mechanism for the gold catalyzed intra-molecular cyclization of 4-pentynoic acid to the corresponding lactone has been suggested by Michelet and coworkers<sup>118</sup>, see **Figure 6.9**.

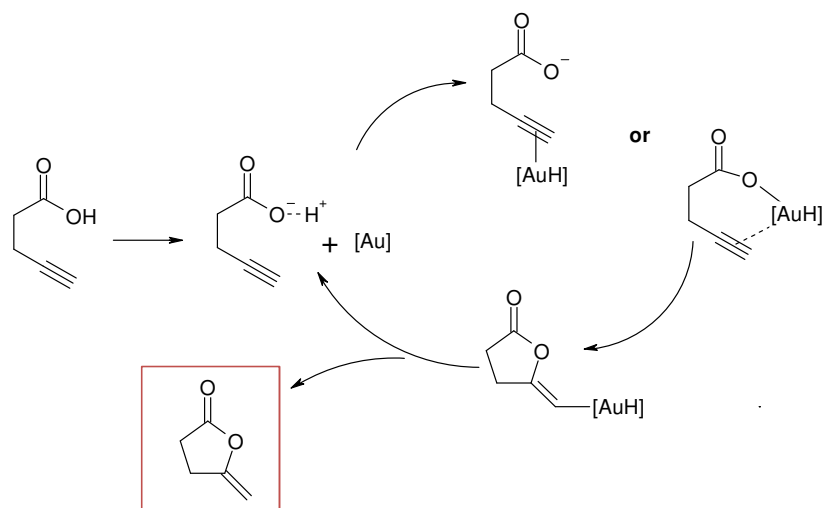


**Figure 6.9** Proposed mechanism of the gold-catalyzed intramolecular cyclization of 4-pentynoic acids to lactones suggested by Michelet and coworkers<sup>118</sup>.

### 6.3 Conclusions and Further Perspectives

Gradients of surface-confined gold and proteins were successfully produced with electrochemistry on the surfaces of particles in the size of  $5\ \mu\text{m}$  by the use of a gold working electrode and a chloride-containing electrolyte. The particle-surface-confined gradients were visualized by coupling thiol-functionalized fluorescent proteins to the gold species. It was found that intra-particle gradients as well as inter-particle gradients could be generated by controlling the length of the potential pulse. Linear gradient of surface-confined  $\text{Au}^{\text{I}}$  was detected with XP spectroscopy on a flat silicon surface when the surface was tilted against the working electrode. The surface-confined  $\text{Au}^{\text{I}}$  species can further be functionalized with thiol-containing molecules to obtain functional gradients, depending on the molecule to be immobilized.

Furthermore, siliceous mesocellular foam (MCF)-heterogenized  $\text{Au}^{\text{I}}$  species were reduced with sodium borohydride to obtain 1-8 nm's gold nanoparticles (AuNPs) well dispersed in the pores of MCF. These heterogenized AuNPs were shown to be highly efficient catalysts at low loadings in the cycloisomerization of 4-pentynoic acids to the

corresponding lactones in the 5-exo style in high yields at RT and with an atmosphere of air. The observed turnover frequencies are the highest reported for catalyzed intra-molecular cyclizations of 4-pentynoic acids in heterogeneous- as well as in homogeneous fashion.

## 7. Highly Dispersed Palladium Nanoparticles on Mesocellular Foam: Efficient and Recyclable Heterogeneous Catalyst for Alcohol Oxidation (Paper VI)

### 7.1 Introduction

The use of molecular oxygen as terminal oxidant in transition metal-catalyzed oxidation reactions has become of particular interest as it circumvents the utilization of the metal catalyst in stoichiometric amounts which is undesirable from both an environmental and economic perspective, see section 1.1.2.1 in this thesis on Palladium Catalysis - Pd(II) Promoted Oxidations. As the activation of O<sub>2</sub> involves a high activation barrier resulting in unsatisfactory activities, efforts have been made in order to solve this problem and a successful example is the biomimetic approach with the use of electron transfer mediators (ETMs) acting as oxygen activators<sup>11</sup>. In heterogeneous catalysis immobilized palladium nanoparticles (PdNPs) have recently been reported as efficient catalysts for the selective oxidation of alcohols with the use of molecular oxygen or air as terminal oxidants<sup>55,119,120</sup>, see section 1.1.3.3 on Transition Metal Nanoparticles.

Siliceous Mesocellular Foams (MCFs) are mesoporous materials with high surface area, high pore volume, and adjustable pore size and with high concentration of surface-confined silanol groups allowing surface modification in order for catalyst immobilizations. The MCFs have shown to be excellent supports for chemical<sup>121</sup>- and bio-catalysts<sup>122</sup> and our group has recently reported on the preparation of PdNPs heterogenized on MCF and demonstrated that it was an efficient heterogeneous catalyst in the racemization of amines<sup>123</sup>. Therefore it was of interest to explore the performance of the PdNPs heterogenized on MCF in the aerobic oxidation of alcohols.

Herein it was found that the heterogeneous PdNP catalysts worked excellent for the oxidations of primary and secondary benzylic alcohols

in aromatic solvents with atmospheric air as terminal oxidant giving turnover numbers (TON) of impressive 450,000 at 160°C. The heterogeneous PdNPs were further shown to be highly stable as it could be used up to 5 times without affecting the turnover numbers.

## *7.2 Results and Discussion*

### *7.2.1 Preparation of Palladium Nanoparticles Heterogenized on Siliceous Mesocellular Foam*

Synthesis of the siliceous mesocellular foam (MCF) has been described elsewhere<sup>124</sup>. Surface-confined silanol groups on the MCF were modified with primary amines by silanization with (3-aminopropyl)trimethoxysilane by refluxing in toluene under inert conditions for 24 hours to obtain MCF-NH<sub>2</sub>, similarly to the previously described thiol-functionalization of silicon surfaces. The amine loading was determined with elemental analysis by nitrogen detection to be approximately 1.5 weight%. Pd(II) was coordinated to the amine ligands by mixing the dispersion of MCF-NH<sub>2</sub> with a homogeneous solution of Li<sub>2</sub>PdCl<sub>4</sub> and the resulting solid (MCF-N-Pd(II)) was washed thoroughly with water and a brown solid was obtained. The MCF heterogenized Pd(II) species were reduced with sodium borohydride to palladium nanoparticles (Pd(0)) whereas the solid shifted from brown to dark brown. An illustration of the overall process employed to produce the MCF heterogenized PdNPs (MCF-N-Pd(0)) is shown in **Figure 7.1**.

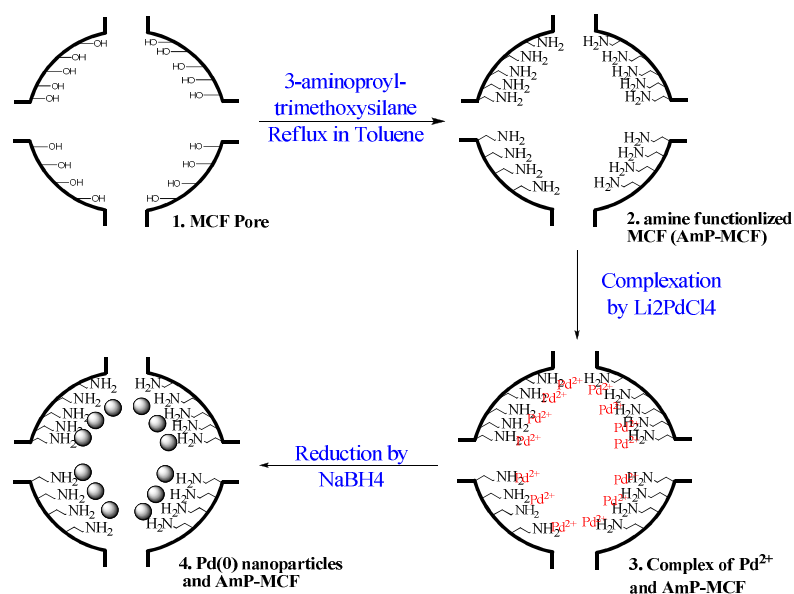


**Figure 7.1** Schematic figure of the preparation of palladium nanoparticles immobilized in the pores of siliceous mesocellular foam.

### 7.2.2 Characterization of Palladium Nanoparticles Heterogenized on Siliceous Mesocellular Foam

The loading of PdNPs heterogenized on MCF were determined with Inductively Coupled Plasma - Mass Spectrometry (ICP-MS) to be 8.25 weight% and the size and oxidation state of the nanoparticles was investigated with Transmission Electron Microscopy (TEM) and X-ray Photoelectron Spectroscopy (XPS) analysis, respectively. TEM image displayed in **Figure 7.2a** showed well dispersed 1-2 nm Pd nanoparticles on MCF with a narrow size distribution. X-ray photoelectron spectra of the Pd  $3d$  doublet recorded before and after reduction of MCF-N-Pd(II) to MCF-N-Pd(0) with  $\text{NaBH}_4$  are displayed in **Figure 7.2b** and **7.2c**, respectively. The shift of the Pd  $3d$  core level signal towards lower binding energies *e.g.* from 337.2 eV to 335.5 eV acquired on the unreduced and the reduced form of Pd(II), respectively, indicating that the majority of the MCF supported Pd(II) is reduced to Pd(0) by the  $\text{NaBH}_4$  treatment.

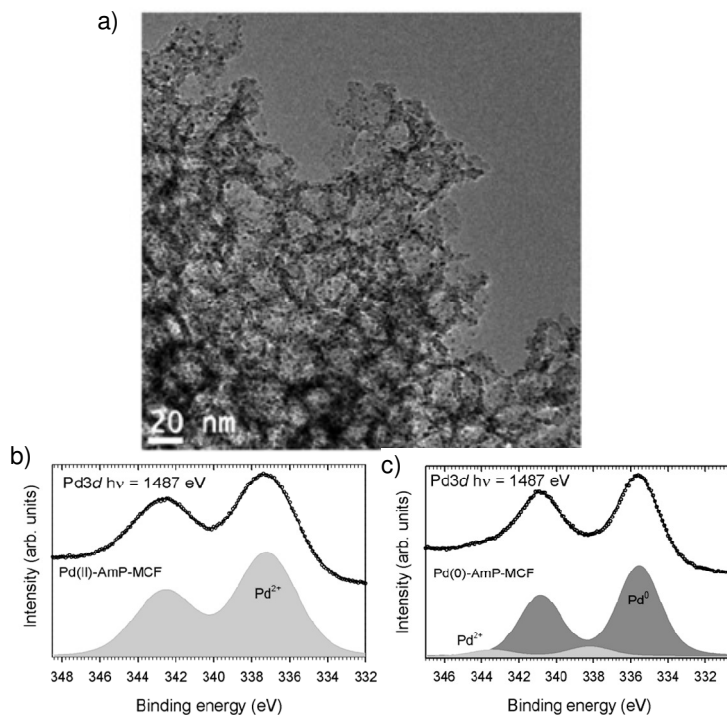


**Figure 7.2** Characterization of the palladium nanoparticles heterogenized on siliceous mesocellular foam. **(a)** TEM image indicating well dispersed Pd nanoparticles in the size of 1-2 nm with a narrow size distribution. **(b)** XPS spectra of the Pd 3d doublet recorded on MCF-N-Pd(II) and **(c)** on MCF-N-Pd(0) catalysts. The shift toward lower binding energies seen for the reduced Pd(II) in **(c)** indicates an reduction of Pd(II) to Pd(0).

### 7.2.3 Aerobic Oxidation of Alcohols by the MCF-N-Pd(0) Catalyst

As a model reaction the aerobic oxidation of 1-phenylethanol to the corresponding ketone 1-phenylethanone (acetophenone) was used in order to optimize the reaction conditions and further also evaluate catalyst activity and recyclability as this substrate was shown to be the most reactive alcohol. It was found that the oxidation works best in aromatic solvents compared to polar aprotic solvents such as acetonitril

and dimethylformamide which can be explained by a coordination of the heteroatom in the polar aprotic solvent to Pd resulting in deactivation of the catalyst consequently yielding low conversions<sup>55,125</sup>. Among the tested aromatic solvents it was found that toluene, *p*-xylene and trifluorotoluene (TFT) were the most suitable solvents for the oxidation. At the end it was found that the most efficient oxidations were run in *p*-xylene at 110°C with atmospheric air as oxidant. Running the reactions for 1 hour in toluene instead of in *p*-xylene differed significantly, with 90% and 99% conversions, respectively. This difference could be explained by the larger steric bulk of *p*-xylene making it less prone to interact with the PdNP surface.

A variety of primary and secondary alcohols were tested as substrates under the reaction conditions described above, where it was found that benzylic- and allylic alcohols showed greater reactivity compared to aliphatic alcohols. This is explained by the ability of benzylic- and allylic alcohols to coordinate to the PdNP surface via  $\pi$ -interactions as proposed previously by Kaneda<sup>55</sup>. Further, it was observed that introduction of substituents on the phenyl ring highly affects the reaction rates of the benzylic substrates. Introduction of bulky- and electron withdrawing substituents was shown to lower the reactivity significantly which most likely is due to less favoured coordination of the substrate to the PdNP surface. However, bulky allylic alcohols were oxidized to their corresponding ketone in high to excellent yields.

Interestingly, with a PdNP catalyst loading of  $1.7 \cdot 10^{-4}$  mol% and at a temperature of 160 °C 1-phenylethanol was oxidized to acetophenone with an impressive turnover number of over 450,000. Compared to previous reports on Pd/Hydroxyapatite (TON=236,000)<sup>55</sup>, Pd/Cerite (TON=250,000)<sup>126</sup>, Au/Cerite (TON=250,000)<sup>127</sup> and Au/Hydrotalcite (TON=200,000)<sup>128</sup> this result is to the best of our knowledge the highest TON reported for this reaction at 160 °C.

The reusability of the MCF-N-Pd(0) catalyst was tested in four recycles. After each run the reaction mixture was centrifuged, the supernatant was recovered, the solid PdNP catalyst was thoroughly washed followed by adding the 1-phenylethanol substrate and increasing the temperature to start the reaction. As shown in **Figure 7.3** the activity of the PdNP catalysts are maintained from the first to the fifth use.

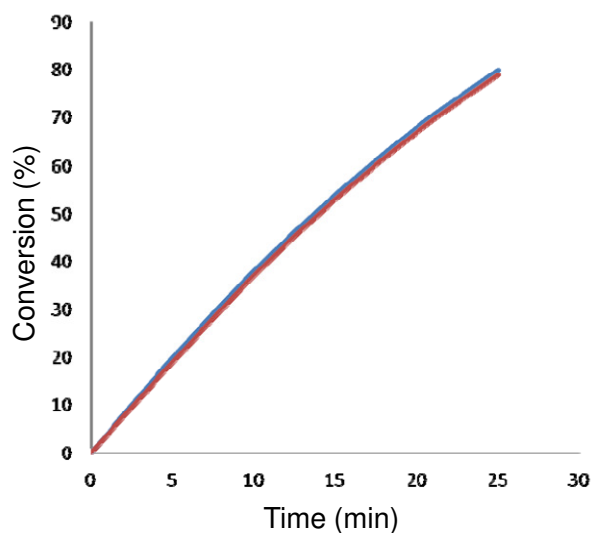


**Figure 7.3** Recyclability study, 1-phenylethanol oxidation by the MCF-N-Pd(0) catalyst at 110 °C in *p*-xylene, (–) the first use and (–) the fifth use.

Further, TEM images of the catalyst before and after the recycling study are displayed in **Figure 7.4** indicating that the heterogenized PdNPs are still well dispersed with preserved shape and size.

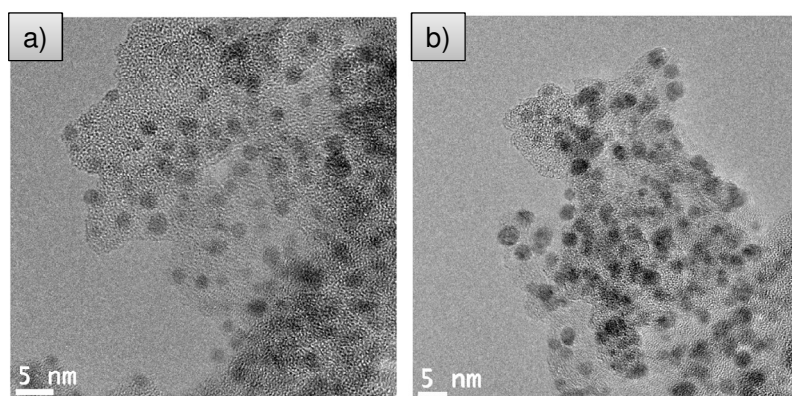


**Figure 7.4** TEM images acquired on the MCF-N-Pd(0) catalyst (a) prior and (b) after recycling.

#### 7.2.3.1 Support Study - Oxidation of 1-Phenylethanol with Pd Nanoparticles Heterogenized on MCF and on Silica

Pd nanoparticles were also produced on ordinary silica with the diameter of 40-60  $\mu\text{m}$  with the same procedure as for the nanoparticle immobilization on the MCF support. The amine content was determined with elemental analysis to be around 1.2 weight% and the Pd loading was determined with ICP-MS to be approximately 8.5 weight% on the silica matrix. TEM analysis indicating PdNPs with broader size distribution on silica than on MCF where the major part of the nanoparticles was in the sizes of 1-2 nm with some bigger particle cluster ranging from 5 to 20 nm, see **Figure 7.5**.

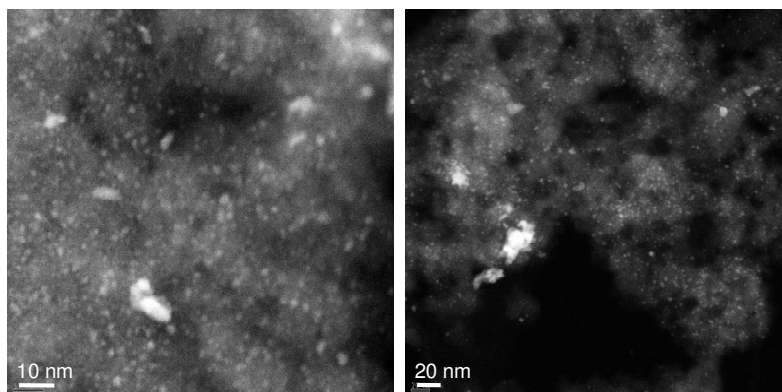
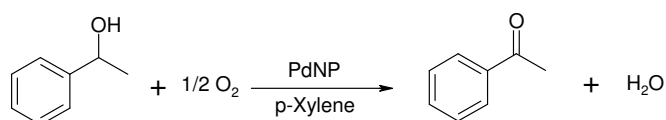


**Figure 7.5** TEM images recorded on PdNPs immobilized on 40-60  $\mu\text{m}$  silica. The Pd nanoparticles have broader size distribution than on MCF where the major part of the particles are in the sizes of 1-2 nm with some bigger particle cluster ranging from 5 to 20 nm. Left 10 nm scale bar and right 20 nm scale bar.

The activity of the Pd(0)-silica nanocatalyst were compared with those of the Pd(0)-MCF in the oxidation of 1-phenylethanol on a 0.8 mmol scale in 2 mL *p*-xylene at 110  $^{\circ}\text{C}$  with atmospheric air as the oxygen source with a concentration of Pd on 3 mol% and 4 mol%, respectively. To evaluate any difference in reusability between the two PdNP supports the catalysts were recycled 3 times. As seen in **Table 7.1** the performance of PdNPs heterogenized on ordinary silica are significantly lower compared to those immobilized on MCF. The conversions after the first use for Pd(0)-silica and Pd(0)-MCF are 95% and 99%, respectively, and whereas the performance of the Pd(0)-MCF is maintained in the 2nd and 3rd use (99%, 98%) the Pd(0)-silica catalyst drops after each use to 84% and 73% conversions after 2nd and 3rd use, respectively. One plausible explanation of the lower activity and reusability of the Pd nanoparticles

immobilized on the silica could be that most of the nanoparticles are confined to an exterior surface whereas on MCF they are confined mainly to an interior surface which would protect the PdNPs from mechanical strain. Therefore nanoparticles on silica could form clusters upon reuse or just leach into the reaction solution thus reducing the number of surface active-sites consequently resulting in lower activity, whereas as observed with TEM, see **Figure 7.4**, PdNPs confined to the inner surface of the pores of MCF are retained in size and shape after several uses.

**Table 7.1** Heterogeneous palladium nanoparticle catalyzed oxidation of 1-phenylethanol to acetophenone.<sup>a</sup>



Pd(0)-MCF (4 mol%)			
No. Of cycles	1	2	3
Conversion (%) <sup>b</sup>	99	99	98
Pd(0)-Silica (3 mol%)			
No. Of cycles	1	2	3
Conversion (%) <sup>b</sup>	95	84	73

<sup>a</sup>. Oxidation of 1-phenylethanol 0.5 mmol at 110 °C with 1 atm air in 2 mL *p*-Xylene. <sup>b</sup>. Conversions determined with GC-MS analysis using ethyl acetate as internal standard.

### 7.3 Conclusions

Well-dispersed palladium nanoparticles in the size of 1-2 nm were heterogenized on MCF via amine ligands. The PdNP - MCF catalysts were shown to be highly efficient in aerobic alcohol oxidations. Benzylic alcohols were oxidized to the corresponding ketones in aromatic solvents with impressive turnover numbers of 450,000 at 160 °C. Further, the Pd nanocatalyst was recycled up to five times with no sign of deactivation

whereas PdNPs immobilized on ordinary silica were observed to lose activity already after the first use.

.

## 8. Concluding Remarks

This thesis addresses the value of surface-confined chemistry for the development of new important functional materials as it focuses on immobilizations of transition metal complexes and shows their potential as useful heterogeneous catalysts and also for the preparation of the exciting anisotropic surfaces.

The two first projects in this thesis deals with the heterogenization of a homogeneous transition metal based oxygen activator namely the tetraphenyl cobalt porphrin (CoTPP) on to flat silicon wafers and on spherical silica particles. Immobilization of the CoTPP catalysts on spherical silica particles was found to circumvent the problem with catalyst deactivation in homogeneous conditions as the activity was increased 100-fold as well as catalyst reusability was obtained. When immobilizations on the silicon wafers were performed, clusters of the catalyst were detected consequently resulting in lower activity than on the silica particles but still higher than the homogeneous counterpart. However, on the silica particles we were only able to achieve low catalyst loadings probably due to a base-promoted disulfide formation during the heterogenization step resulting in a polymerization of the CoTPP molecules in solution. For scale-up purposes it is therefore desirable to increase these catalyst loadings significantly.

In the next two projects we developed a method based on electrochemical site-specific oxidations for the preparation of anisotropic surfaces where surface-confined reactive patches and gradients of gold species were produced on particles on a large scale whereas  $10^6$  particles were modified in a single step. The particle-surface-confined patches and gradients were conjugated with proteins to obtain fluorescence and the gold species could be used for a straightforward immobilization of the thioacetate functionalized CoTPPs thus generating a monolayer distribution of the catalyst as seen on gold surfaces subsequently increasing the low loading of CoTPP on particles. For more applications in heterogeneous catalysis, the reactive patches can further be functionalized in order to obtain bimetallic catalysts with particles-on-particle morphology whereas the gold functionalized particles were demonstrated to be efficient catalysts in cycloisomerizations of 4-alkynoic acids to lactones.

In the final project we describe the synthesis of heterogenized palladium nanoparticles (PdNPs) well dispersed in the pores of amine-modified mesocellular foam (MCF). The MCF heterogenized PdNPs were shown to be a highly efficient catalyst for the aerobic oxidations of allylic- and benzylic alcohols in aromatic solvents. Impressive turnover numbers of 450,000 could be obtained together with maintained activity upon reuse whereas PdNPs immobilized on ordinary silica were observed to lose activity already after the first use.

The projects explored in this thesis shows the potential to improve outside the world of academia as project II has been awarded the Pfizer Prize for the best diploma work in biotechnology in 2008 whereas project III was awarded the Ångström Materials Academy Innovation Prize in 2009 together with a granted European patent.

# Appendix A

## Contribution to Publications I - VI

- I.** Performed the immobilization of the catalyst and the activity tests. Took part in the AFM measurements and the writing of the article.
- II.** All experimental works and participate in the XPS analysis. Wrote the manuscript.
- III.** All experimental works and participate in the XPS analysis. Wrote the article.
- IV.** All experimental works and participate in the XPS analysis. Wrote the article.
- V.** Prepared the catalyst and took part in the cycloisomerizations. Wrote the manuscript.
- VI.** Participate in the XPS measurements and prepared the Pd catalyst on silica and performed the support study. Took part in the writing of the manuscript.

## Appendix B

### Reprint Permissions

Reprint permissions were granted for each publication by the following publishers:

- I.** K. L. E. Eriksson, W. W. Y. Chow, C. Puglia, J.-E. Bäckvall, E. Göthelid, S. Oscarsson, *Langmuir* **2010**, 26, 16349. Copyright © 2010, American Chemical Society.
- II.** -
- III.** K. Eriksson, L. E. Johansson, E. Göthelid, L. Nyholm, S. Oscarsson, *J. Mater. Chem.*, **2012**, 22, 7681. Copyright © 2012, Royal Society of Chemistry.
- IV.** K. Eriksson, P. Palmgren, L. Nyholm, S. Oscarsson, *Langmuir* **2012**, 28, 10318. Copyright © 2012, American Chemical Society.
- V.** -
- VI.** E. V. Johnston, O. Verho, M. D. Kärkäs, M. Shakeri, C.-W. Tai, P. Palmgren, K. Eriksson, S. Oscarsson, J.-E. Bäckvall. *Chem. Eur. J.*, **2012**, 18, 12202. Copyright © 2012 WILEY-VCH Verlag GmbH & Co. KGaA, Weinheim.

# Acknowledgements

I would like to express my sincerest gratitude to the following people:

My supervisors,

*Prof. Sven Oscarsson* for wonderful guidance through this time in prosperity and adversity. Thank you for you always believes in my own ideas and for letting me explore them in my own ways. What a journey!

*Prof. Jan-Erling Bäckvall* for accepting me as a Ph. D candidate in your group and for you finding my projects interesting.

My coworkers,

The Ångström Laboratory gang at Uppsala University: *Rebecca Stjernberg Bejhed, Klas Gunnarsson, Prof. Peter Svedlindh, Prof. Leif Nyholm, Rimantas Brucas, Emmanuelle Göthelid* and *Carla Puglia*. It has been a pleasure to work with you.

*Oscar Verho* for your impressive work on the Au-catalyzed cycloisomerizations.

My own “office girls” *Bao-Lin Lee* and *Tanja Laine* for making the office so much nicer.

Former members of *Sven Oscarssons* group: *Cecilia Granstam, Charlotte Nilsson, LarsErik Johansson, Winnie Chow, Alessandro Surpi, Greger Ledung* and *Erika Ledung*.

*Dr. Andreas Persson* for helping me with the advanced organic synthesis course.

*Richard Lihammar* the professional “fume-hood police”. Thank you!

The LOAB team, especially *Björn Strandwitz*.

To them outside the world of academia and research,

My dear family, för allt ert stöd och intresse i det jag gör fastän jag sällan kan förklara vad det är jag håller på med, *Mamma, Pappa, syskon* och övrig *släkt* och *vänner*. Ni vet vilka ni är!

My friends!

Everyone I have met in the forest during the years! I can't bring up you all but I think we will meet again when the leaves start to fall and the dogs start to woof.

My dogs, Cessi, Nellie (Baronessan) and Raya!

Finally,

My true love, *Linett Carlsson*! I love you quite a lot.



## References

- 
- <sup>1</sup> Z. W. Seh, S. Liu, M. Low, S.-Y. Zhang, Z. Liu, A. Mlayah, M.-Y. Han, *Adv. Mater.* **2012**, *24*, 2310.
- <sup>2</sup> S. J. Ebbens, J. R. Howse, *Langmuir*, **2011**, *27*, 12293.
- <sup>3</sup> J. J. Berzelius, *Ann. Chem. et. Phys.*, **1836**, *61*, 146.
- <sup>4</sup> P. Atkins, J. De Paula, *Atkins Physical Chemistry*, 7<sup>th</sup> ed.; Oxford University Press: New York, **2000**, pp 830-861.
- <sup>5</sup> A. Schmid, J. S. Dordick, B. Hauer, A. Kiener, M. Wubbolts, B. Witholt, *Nature*, **2001**, *409*, 258.
- <sup>6</sup> R. H. Crabtree, *The Organometallic Chemistry of the Transition Metals*, 4<sup>th</sup> ed.; John Wiley and Sons: New Jersey, **2005**.
- <sup>7</sup> J. Smidt, W. Hafner, R. Jira, S. Sedlmeier, R. Sieber, R. Ruttinger, H. Kojer, *Angew. Chem.* **1959**, *71*, 176-182.
- <sup>8</sup> A. de Meijere, F. Diederich, *Metal-Catalyzed Cross-Coupling Reactions*; Wiley-VCH: Weinheim, **2004**; *1*, Chapters 1-6.
- <sup>9</sup> S. S. Stahl, *Angew. Chem. Int. Ed.* **2004**, *43*, 3400-3420.
- <sup>10</sup> P. Anastas, N. Eghbali, *Chem. Soc. Rev.*, **2010**, *39*, 301.
- <sup>11</sup> J.-E. Bäckvall, A.K. Awasthi, Z.D. Renko, *J. Am. Chem. Soc.* **1987**, *109*, 4750.
- <sup>12</sup> J. Piera, J.-E. Bäckvall, *Angew. Chem. Int. Ed.* **2008**, *47*, 3506.
- <sup>13</sup> J. Piera, K. Närhi, J.-E. Bäckvall, *Angew. Chem. Int. Ed.* **2006**, *45*, 6914.
- <sup>14</sup> H. Grennberg, S. Faizon, J.-E. Bäckvall, *Angew. Chem. Int. Ed.* **1993**, *32*, 263.
- <sup>15</sup> J.-E. Bäckvall, R.B. Hopkins, H. Grennberg, M.M. Mader, A.K. Awasthi, *J. Am. Chem. Soc.* **1990**, *112*, 5160-5166.
- <sup>16</sup> J. M. Thomas, *Angew. Chem. Int. Ed.* **1994**, *33*, 913.
- <sup>17</sup> P. Sabatier, J. B. Senderens, *Comp. Rendus.* **1899**, *128*, 1173.
- <sup>18</sup> J. Wisniak, *Indian J. Chem. Technol.* **2005**, *12*, 232.
- <sup>19</sup> G. Ertl, *J. Vac. Sci. Technol. A*, **1983**, *1*, 1247.

- 
- <sup>20</sup> R. Imbihl, R.J. Behm, G. Ertl, W. Moritz, *Surf. Sci.* **1982**, 123, 129-140.
- <sup>21</sup> G. Ertl, *Science*, **1991**, 254, 1750.
- <sup>22</sup> T. Enzel, G. Ertl, *Adv. Catal.* **1979**, 28, 1.
- <sup>23</sup> P. Forzatti, L. Lietti, *Catal. Today*, **1999**, 52, 165.
- <sup>24</sup> G. Ertl, M. Weiss, S.B. Lee, *Chem. Phys. Lett.* **1979**, 60, 391.
- <sup>25</sup> D. R. Strongin, G. A. Somorjai, *J. Catal.* **1988**, 109, 51.
- <sup>26</sup> J. Segner, C.T. Campbell, G. Doyen, G. Ertl, *Surf. Sci.* **1984**, 138, 505.
- <sup>27</sup> M. D. Graham, M. Bar, I. G. Kevrekidis, K. Asakura, J. Lauterbach, H.-H. Rotermund, G. Ertl, *Phys. Rev. E*, **1995**, 52, 76.
- <sup>28</sup> S. L. Bernasek, G. A. Somorjai, *Surf. Sci.*, **1975**, 48, 204.
- <sup>29</sup> D. W. Blakely, G. A. Somorjai, *J. Catal.*, **1976**, 42, 181.
- <sup>30</sup> R. Burch and A.R. Flambard, *J. Catal.*, **1982**, 86, 384.
- <sup>31</sup> A. Boffa, C. Lin, A.T. Bell, G.A. Somorjai, *J. Catal.*, **1994**, 149, 149.
- <sup>32</sup> A. Zsigmond, F. Notheisz, J.-E. Bäckvall, *Catal. Lett.* **2000**, 65, 135.
- <sup>33</sup> J. Reedijk, E. Bouwman, editors. **1999**. *Bioorganic catalysis* Vol. Marcel Dekker Incorporated, New York, NY, USA.
- <sup>34</sup> M. Bergkvist, J. Carlsson, S. Oscarsson, *J. Biomed. Mater. Res. A*, **2003**, 64, 349.
- <sup>35</sup> E. Katchalki-Katzir, *Trends Biotechnol.* **1993**, 1, 471.
- <sup>36</sup> F. Basolo, B. M. Hoffman, J. A. Ibers, *Acc. Chem. Res.*, **1975**, 8, 384.
- <sup>37</sup> A. L. Balch, M. Mazzanti, T. N. StClaire, M. M. Olmstead, *Inorg. Chem.*, **1995**, 34, 2194.
- <sup>38</sup> I. O. Benitez, B. Bujoli, L. J. Camus, C. M. Lee, F. Odobel, D. R. Talham, *J. Am. Chem. Soc.* **2002**, 124, 4363.
- <sup>39</sup> C.C. Guo, G. Huang, X.B. Zhang, D.C. Guo, *Appl. Catal. A Gen.*, **2003**, 247, 261.
- <sup>40</sup> A. H. Éll, G. Csornyik, V. F. Slagt, J.-E. Bäckvall, S. Berner, C. Puglia, G. Ledung, S. Oscarsson, *Eur. J. Org. Chem.*, **2006**, 1193-1199.
- <sup>41</sup> S. Berner, S. Biela, G. Ledung, A. Gogoll, J.-E. Bäckvall, C. Puglia, S. Oscarsson, *J. Catal.*, **2006**, 244, 86.
- <sup>42</sup> D. Astruc, F. Lu, J. R. Aranzaes, *Angew. Chem. Int. Ed.*, **2005**, 44, 7852.
- <sup>43</sup> M. E. Grass, Y. Zhang, D. R. Butcher, J. Y. Park, Y. Li, H. Bluhm, K. M. Bratlie, T. Zhang, G. A. Somorjai, *Angew. Chem. Int. Ed.*, **2008**, 47, 8893.

- 
- <sup>44</sup> M. A. R. Meier, M. Filali, J.-F. Gohy, U. S. Schubert, *J. Mater. Chem.*, **2006**, *16*, 3001.
- <sup>45</sup> G. J. Hutchings, *J. Catal.* **1985**, *96*, 292.
- <sup>46</sup> M. Haruta, T. Kobayashi, H. Sano, N. Yamada, *Chem. Lett.* **1987**, *16*, 405.
- <sup>47</sup> L. Prati, M. Rossi, *J. Catal.* **1998**, *176*, 552.
- <sup>48</sup> M. D. Hughes, Y.-J. Xu, P. Jenkins, P. McMorn, P. Landon, D. I. Enache, A. F. Carley, G. A. Attard, G. J. Hutchings, F. King, E. H. Stitt, P. Johnston, K. Griffin, C. J. Kiely, *Nature*, **2005**, *437*, 1132.
- <sup>49</sup> M. Haruta, *Nature*, **2005**, *437*, 1098.
- <sup>50</sup> A. S. K. Hashmi, G. J. Hutchings, *Angew. Chem. Int. Ed.* **2006**, *45*, 7896.
- <sup>51</sup> S. Biela, M. Rossi, *Chem. Commun.* **2003**, 378.
- <sup>52</sup> S. Biela, G. L. Castiglioni, C. Fumagalli, L. Prati, M. Rossi, *Catal. Today*, **2002**, *72*, 43.
- <sup>53</sup> M. Okumura, S. Nakamura, S. Tsubota, T. Nakamura, M. Azuma, *Catal. Lett.* **1998**, *51*, 53.
- <sup>54</sup> M. Okumura, T. Akita, M. Haruta, *Catal. Today*, **2002**, *74*, 265.
- <sup>55</sup> K. Mori, T. Hara, T. Mizugaki, K. Ebitani, K. Kaneda, *J. Am. Chem. Soc.* **2004**, *126*, 10657.
- <sup>56</sup> X. R. Ye, Y.-H. Lin, C. M. Wai, *Chem. Commun.* **2003**, 642.
- <sup>57</sup> J. Huang, T. Jiang, H.-X. Gao, B.-X. Han, Z.-M. Liu, W.-Z. Wu, Y.-H. Chang, G.-Y. Zhao, *Angew. Chem.* **2004**, *116*, 1421.
- <sup>58</sup> J. G. de Vries, A. H. M. de Vries, *Eur. J. Org. Chem.* **2003**, 799.
- <sup>59</sup> K. Wada, K. Yano, T. Kondo, T. Mitsudo, *Catal. Today* **2006**, *117*, 242.
- <sup>60</sup> D. Rodríguez-Fernández, L. M. Liz-Marzán, *Part. Part. Syst. Charact.* **2013**, *30*, 46-60.
- <sup>61</sup> C. Casagrande, P. Fabre, E. Raphaël, M. Veyssie, *Europhys. Lett.* **1989**, *9*, 251.
- <sup>62</sup> P. de Gennes, *Angew. Chem. Int. Ed.* **1992**, *31*, 842.
- <sup>63</sup> J. Du, R. K. O'Reilly, *Chem. Soc. Rev.* **2011**, *40*, 2402-2416.
- <sup>64</sup> M. Lattuada, T. A. Hatton, *Nano Today* **2011**, *6*, 286.
- <sup>65</sup> M. Feyen, C. Weidenthaler, F. Schüth, A. -H. Lu, *J. Am. Chem. Soc.* **2010**, *132*, 6791.
- <sup>66</sup> T. Nisisako, T. Torii, T. Takahashi, Y. Takizawa, *Adv. Mater.* **2006**, *18*, 1152.

- 
- <sup>67</sup> S. Lone , S. H. Kim , S. W. Nam , S. Park , I. W. Cheong , *Langmuir* **2010**, *26*, 17975 .
- <sup>68</sup> D. M. Andala, S. H. R. Shin, H. -Y. Lee, K. J. M. Bishop, *ACS Nano*, **2012**, *6*, 1044.
- <sup>69</sup> A. Wolf, A. Walther, A. H. E. Müller, *Macromolecules* **2011**, *44*, 9221.
- <sup>70</sup> O. Cayre, V. N. Paunov, O. D. Velev, *J. Mater. Chem.*, **2003**, *13*, 2445–2450.
- <sup>71</sup> N. Glaser, D. J. Adams, A. Boker, G. Krausch, *Langmuir* **2006**, *22*, 5227-5229.
- <sup>72</sup> A. Walther, M. Hoffmann, A.H.E. Muller, *Angew. Chem. Int. Ed.* **2008**, *47*, 711-714.
- <sup>73</sup> C. Xu, B. Wang, S. Sun, *J. Am. Chem. Soc.* **2009**, *131*, 4216.
- <sup>74</sup> S. Birtwell and H. Morgan, *Integr. Biol.*, **2009**, *1*, 345-362.
- <sup>75</sup> M. Dejneka, A. Streltsov, S. Pal, A. Frutos, C. Powell, K. Yost, P. Yuen, U. Muller, J. Lahiri, *Proc. Natl. Acad. Sci. U. S. A.*, **2003**, *2*, 389.
- <sup>76</sup> C. Wang, H. Yin, S. Dai, S. Sun, *Chem. Mater.* **2010**, *22*, 3277.
- <sup>77</sup> B. D. Gates, Q. Xu, M. Stewart, D. Ryan, C. G. Willson, G. M. Whitesides, *Chem. Rev.* **2005**, *105*, 1171.
- <sup>78</sup> A. W. Flounders, D. L. Brandon, A. H. Bates, *Appl. Biochem. Biotechnol.* **1995**, *50*, 265.
- <sup>79</sup> J. Zou, S. M. Kauzlarich, *J. Clust. Sci.* **2008**, *19*, 341-355.
- <sup>80</sup> M. Vigano, R. Suriano, M. Levi, S. Turri, M. Chiari, F. Damin, *Surf. Sci.* **2007**, *601*, 1365-1370.
- <sup>81</sup> E. Verne', C. Vitale-Brovarone, E. Bui, C. L. Bianchi, A. R. Boccaccini, *J. Biomedical Materials Research A.* **2009**, 981-992.
- <sup>82</sup> Y. Chen, L. Jallo, M. A. S. Quintanilla, R. Dave, *Colloids and Surfaces A: Physicochem. Eng. Aspects*, **2010**, *361*, 66-80.
- <sup>83</sup> X. Zong, C. Wu, X. Wu, Y. Lu, P. Wang, *J Zhejiang Univ Sci B*, **2009**, *10* (11) 860-866.
- <sup>84</sup> W. W. Cleland, *Biochemistry*, **1964**, *3*, 480-482.
- <sup>85</sup> J. Carlsson, H. Drevin, R. Axen, *Biochem. J.* **1978**, *173*, 723-737.
- <sup>86</sup> K. Brocklehurst, J. Carlsson, M. P. J. Kierstan, E. M. Crook, *Biochem. J.*, *133*, **1973**, 573-584.
- <sup>87</sup> R. G Nuzzo, D. L. Allara, *J. Am. Chem. Soc.* **1983**, *105*, 4481.
- <sup>88</sup> E. B. Troughton, C. D. Bain, G. M. Whitesides, D. L. Allara, M. D. Porter, *Langmuir* **1988**, *4*, 365.
- <sup>89</sup> A. Ihs, K. Uvdal, B. Liedberg, *Langmuir* **1993**, *9*, 733.

- 
- <sup>90</sup> J. A. Mielczarski, R. H. Yoon, *Langmuir* **1991**, 7, 101.
- <sup>91</sup> M. W. Walczak, C. Chung, S. M. Stole, C. A. Widrig, M. D. Porter, *J. Am. Chem. Soc.* **1991**, 113, 2370.
- <sup>92</sup> C. A. Widrig, C. Chung, M. D. Porter, *J. Electroanal. Chem.* **1991**, 310, 335.
- <sup>93</sup> Y. Li, J. Huang, R. T. McIver, J. C. Hemminger, *J. Am. Chem. Soc.* **1992**, 114, 2428.
- <sup>94</sup> L. H. Dubois, R. G. Nuzzo, *Ann. Phys. Chem.* **1992**, 43, 437.
- <sup>95</sup> A. Demoz, D. J. Harrison, *Langmuir* **1993**, 9, 1046.
- <sup>96</sup> A. Ulman, *J. Mater. Educ.* **1989**, 11, 205.
- <sup>97</sup> K. Shimazu, Y. Sato, I. Yagi, K. Uosaki, *Bull. Chem. Soc. Jpn.* **1994**, 67, 863.
- <sup>98</sup> M. Stratmann, *Adv. Mater.* **1990**, 2, 191.
- <sup>99</sup> A. J. Bard, L. R. Faulkner, *Electrochemical Methods: Fundamentals and Applications*; Wiley: New York, **2001**, pp 580-631.
- <sup>100</sup> M. Brust, M. Walker, D. Bethell, D. J. Schiffrin, R. Whyman, *J. Chem. Soc. Chem. Commun.* **1994**, 801.
- <sup>101</sup> A. J. Bard, L. R. Faulkner, *Electrochemical Methods: Fundamentals and Applications*; Wiley: New York, **2001**, pp 1.
- <sup>102</sup> F. Batista-Viera, M. Barbieri, K. Ovsejevi, C. Manta, J. Carlsson, *Appl. Biochem. Biotechnol.*, **1991**, 31, 175.
- <sup>103</sup> E. Pavlovic, A. P. Quist, U. Gelius, L. Nyholm, S. Oscarsson, *Langmuir* **2003**, 19, 4217-4221.
- <sup>104</sup> E. Pavlovic, A. P. Quist, L. Nyholm, A. Pallin, U. Gelius, S. Oscarsson, *Langmuir* **2003**, 19, 10267-10270.
- <sup>105</sup> E. Pavlovic, S. Oscarsson, A. P. Quist, *Nano Lett.*, **2003**, 3, 779.
- <sup>106</sup> A. L. Kieran, A. D. Bond, A. M. Belenguer, J. K. M. Sanders, *Chem. Commun.* **2003**, 12, 2674.
- <sup>107</sup> J. Podesta, R. C. V. Piatti, A. J. Arvia, *Electrochim. Acta*, **1979**, 24, 633.
- <sup>108</sup> P. H. Qi, J. B. Hiskey, *Hydrometallurgy*, **1993**, 32, 161.
- <sup>109</sup> A. McNeillie, D. H. Brown, W. E. Smith, *J. C. S. Dalton*, **1980**, 767.
- <sup>110</sup> A. J. Bard, L. R. Faulkner, *Electrochemical Methods: Fundamentals and Applications*; Wiley: New York, **2001**, pp 147.
- <sup>111</sup> E. V. Johnston, O. Verho, M. D. Kärkäs, M. Shakeri, C.-W. Tai, P. Palmgren, K. Eriksson, S. Oscarsson, J.-E. Bäckvall. *Chem. Eur. J.*, **2012**, 18, 12202.

- 
- <sup>112</sup> Y. Hu, Y. Song, Y. Wang, J. Di, *Thin Solid Films*, **2011**, 519, 6605.
- <sup>113</sup> H. Tsunoyama, H. Sakurai, Y. Negishi, T. Tsukuda, *J. Am. Chem. Soc.* **2005**, 127, 9374.
- <sup>114</sup> F. Neatu, K. Triantafyllidis, J.-P. Genet, V. Michelet, V. I. Parvulescu, *Stud. Surf. Sci. Catal.* **2008**, 174, 1057.
- <sup>115</sup> F. Neatu, Z. Li, R. Richards, P. Y. Toullec, J.-P. Genet, K. Dumbuya, J. M. Gottfried, H.-P. Steinbrück, V. I. Parvulescu, V. Michelet, *Chem. Eur. J.* **2008**, 14, 9412.
- <sup>116</sup> F. Neatu, L. Protesescu, M. Florea, V. I. Parvulescu, C. M. Teodorescu, N. Apostol, P. Y. Toullec, V. Michelet, *Green Chem.* **2010**, 12, 2145.
- <sup>117</sup> H. Harkat, A. Y. Dembele, J.-M. Weibel, A. Blanc, P. Pale, *Tetrahedron*, **2009**, 65, 1871.
- <sup>118</sup> F. Neatu, V. I. Parvulescu, V. Michelet, J.-P. Genet, A. Goguet, C. Hardacre, *New J. Chem.*, **2009**, 33, 102.
- <sup>119</sup> Y. Uozumi, R. Nakao, *Angew. Chem. Int. Ed.* **2003**, 345, 103.
- <sup>120</sup> Y. Pérez, M. L. Ruiz-González, J. M. González-Calbet, P. Concepción, M. Boronat, A. Corma, *Catal. Today* **2012**, 180, 59.
- <sup>121</sup> D. Astruc, *Inorg. Chem.* **2007**, 1884.
- <sup>122</sup> M. Shakeri, K. Engström, A. Sandström, J.-E. Bäckvall, *ChemCatChem*, **2010**, 2, 534.
- <sup>123</sup> M. Shakeri, C.-W. Thai, E. Göthelid, S. Oscarsson, J.-E. Bäckvall, *Chem. Eur. J.* **2011**, 17, 13269.
- <sup>124</sup> Y. Han, S. S. Lee, J. Y. Ying, *Chem. Mater.* **2006**, 18, 643.
- <sup>125</sup> R. A. Sheldon, I. W. C. E. Arends, G. J. ten Brink, A. Dijkstra, *Acc. Chem. Res.* **2002**, 35, 774.
- <sup>126</sup> A. Abad, C. Almela, A. Corma, H. Garcia, *Tetrahedron* **2006**, 62, 6666.
- <sup>127</sup> T. Mitsudome, A. Noudjima, T. Mizugaki, K. Jitsukawa, K. Kaneda, *Adv. Synth. Catal.* **2009**, 351, 1890.
- <sup>128</sup> A. Abad, P. Concepción, A. Corma, H. Garcia, *Angew. Chem.* **2005**, 117, 4134; *Angew. Chem. Int. Ed.* **2005**, 44, 4066.